GelNB molecular coating as a biophysical barrier to isolate intestinal irritating metabolites and regulate intestinal microbial homeostasis in the treatment of inflammatory bowel disease

Qijiang Mao [a,b,c,1], Haoqi Pan [a,1], Yiyin Zhang [a,1], Yi Zhang [d,e,1], Qiuwen Zhu [d,e], Yi Hong [d,e], Zhengze Huang [b], Yang Li [f], Xu Feng [a], Yifeng Fang [a], WenChao Chen [a], Pengfei Chen [g], Bo Shen [a,b,*], Hongwei Ouyang [d,e,**], Yuelong Liang [a,b,c,***]

[a] Department of General Surgery, Sir Run Run Shaw Hospital, Zhejiang University School of Medicine, Hangzhou, 310016, China
[b] Key Laboratory of Laparoscopic Technology of Zhejiang province, Hangzhou, 310016, China
[c] Zhejiang Province Medical Research Center of Minimally Invasive Diagnosis and Treatment of Abdominal Diseases, Hangzhou, 310028, China
[d] Dr. Li Dak Sum & Yip Yio Chin Center for Stem Cells and Regenerative Medicine, Department of Orthopedic Surgery of the Second Affiliated Hospital, Zhejiang University School of Medicine, Hangzhou, China
[e] Zhejiang University-University of Edinburgh Institute, Zhejiang University School of Medicine, Key Laboratory of Tissue Engineering and Regenerative Medicine of Zhejiang Province, Zhejiang University School of Medicine, Hangzhou, China
[f] The State Key Laboratory of Fluid Power and Mechatronic Systems, School of Mechanical Engineering, Zhejiang University, Hangzhou, 310028, China
[g] Department of Orthopaedic Surgery, Sir Run Run Shaw Hospital, Medical College of Zhejiang University, Hangzhou, Zhejiang, 310016, China

ARTICLE INFO

ABSTRACT

Inflammatory bowel disease (IBD) is a chronic, immune-mediated inflammatory disease characterized by the destruction of the structure and function of the intestinal epithelial barrier. Due to the poor remission effect and severe adverse events associated with current clinical medications, IBD remains an incurable disease. Here, we demonstrated a novel treatment strategy with high safety and effective inflammation remission via tissue-adhesive molecular coating. The molecular coating is composed of o-nitrobenzaldehyde (NB)-modified Gelatin (GelNB), which can strongly bond with $-NH_2$ on the intestinal surface of tissue to form a thin biophysical barrier. We found that this molecular coating was able to stay on the surface of the intestine for long periods of time, effectively protecting the damaged intestinal epithelium from irritations of external intestinal metabolites and harmful flora. In addition, our results showed that this coating not only provided a beneficial environment for cell migration and proliferation to promote intestinal repair and regeneration, but also achieved a better outcome of IBD by reducing intestinal inflammation. Moreover, the *in vivo* experiments showed that the GelNB was better than the classic clinical medication—mesalazine. Therefore, our molecular coating showed potential as a promising strategy for the prevention and treatment of IBD.

1. Introduction

Inflammatory bowel disease (IBD) is a chronic, immune-mediated inflammatory disease [1,2], including ulcerative colitis (UC) and Crohn's disease (CD). In recent years, with changes in diet structure, the incidence of IBD has increased worldwide, and is predicted to reach 1% by 2030 [3]. Patients with IBD often present with symptoms such as chronic abdominal pain, fever, intestinal obstruction or diarrhea, mucus, pus, and blood stool, and often suffer from unbearable pain due to repeated attacks of the disease [4]. More seriously, IBD increases the

occurrence of colorectal cancer 2 to 8 times in patients with CD than in healthy individuals [5]. Currently, there are no targeted drugs available for the treatment of IBD, and clinically, supportive treatment is the main treatment strategy. 5-amino salicylic acid (5-ASA) and adrenal cortex hormones are more common in patients with mild-to-moderate illness. However, 20% of patients develop severe illnesses and require surgical resection [6].

As for the traditional anti-inflammatory drug 5-ASA (also known as mesalazine), the main mechanism of action is the delivery of the active ingredient mesalazine to the target site and anti-inflammation. However, this treatment may only induce sustained remission in a small number of patients [7]. Corticosteroids are mainly used in the acute phase of treatment, but long-term use can lead to many side effects, seriously reducing the quality of the patients' lives [8]. Anti-tumor necrosis factor (TNF) drugs and $\alpha 4\beta 7$ integrin blocker vedolizumab are also widely used in clinical applications, but serious complications such as infection and malignancies have been reported, and larger clinical trials are required to confirm its safety [9–12]. In addition, systemic administration increases the burden on various organs [13]. Therefore, the development of a new strategy that is able to not only facilitate the healing of mucosal and tissue, but also relieve the inflammation level and minimize side effects is of great clinical significance and economic value [14].

The most obvious feature of IBD is the destruction of the intestinal epithelial barrier structure and function [15]. Although the specific pathogenesis of IBD remains unclear, one possible mechanism is that the stimulation of external factors (such as food) reduces the synthesis of mucin 2 (a characteristic protein in the colonic mucus layer), which leads to the destruction of intestinal barrier function, enabling more digestive tract metabolites and intestinal microbes to cross the barrier and induce inflammatory action. For example, the excessive exchange of metabolites, such as glucose, can induce the activation of natural killer T cells and M1 macrophages [16,17]. The interleukin-13 (IL-13) released by these inflammatory cells upon activation has been shown to induce barrier dysfunction [18]. IBD is closely related to intestinal micro-ecology. Once the immune system deteriorates, the abnormal response to the intestinal microflora leads to a series of inflammatory events, which results in damage to the intestinal wall, causing intestinal mucosal barrier breakdown and accelerating the progression of IBD. IBD patients often suffer from intestinal microflora disorders, including changes in microbial components (such as the reduction in microbial diversity, loss of *Bacteroides* and *Firmicutes*, and the appearance of *Clostridium*), and alterations in microbial metabolic function (such as a decrease in short-chain fatty acids as well as butyric acid, and an increase in oxidative stress) [19,20]. Therefore, the isolation of external stimuli and the regulation of intestinal microecology are potential solutions for IBD treatment.

Here, we propose a strategy for isolating external stimuli and regulating intestinal microecology through "molecular coating." In a previous study, we prepared a molecular coating that could recruit cells and promote corneal repair [21]. This molecular coating is composed of o-nitrobenzaldehyde (NB)-modified Gelatin (GelNB), which can strongly bond with –NH₂ on the tissue surface via photogenerated aldehyde groups after ultraviolet light (UV) activation [22]. Based on this, we predicted that this molecular coating could act as a biophysical barrier on the intestinal mucosa, not only blocking the irritation of metabolites through the protection of the physical barrier, resulting in the activation of inflammatory cells, such as macrophages transformation from M1 to M2 [23], but also acting as a biological barrier by adjusting the intestinal flora to maximize the therapeutic effect of IBD.

In this study, we investigated the *in vitro* and *in vivo* effects of GelNB molecular coating in order to achieve the long-term protection of the damaged intestinal tract. First, the formation and long-term retention performance of GelNB molecular coating was verified, and the physical barrier function of GelNB was confirmed to eliminate the intestinal irritant metabolites to a large extent. We then characterized the prophylactic and therapeutic effects of GelNB molecular coating on IBD model mice. All the indicators suggested that the effect of GelNB was significantly more efficient and safer than that of mesalazine. Moreover, the levels of inflammatory factors and cell tight junction proteins also confirmed the excellent anti-inflammatory effect and physical barrier function of the molecular coating. Finally, 16S sequencing was performed to analyze the transformation of intestinal flora and to explore the potential underlying mechanisms of IBD repair from the perspective of biological barriers. In conclusion, the GelNB molecular coating can achieve ideal local adhesion in the intestinal tract, playing a biophysical barrier role in the damaged intestinal tract, which has promising prospects for applications in the prevention and treatment of IBD (Fig. 1).

2. Results and discussion

2.1. Properties and physical barrier action of GelNB molecular coating

Traditional hydrogels have unique advantages in the application of local wound treatment. However, they also have many limitations when applied to IBD, such as low bioavailability, non-specific tissue distribution, rapid elimination, and poor colon retention [24–26]. Our "GelNB molecular coating" was confirmed to have outstanding adhesion performance, long-term retention performance, and convenient usage [21]. GelNB was dissolved in water and directly injected into the intestine after being activated by UV light. Through *in vitro* gelling experiments, we found that the GelNB solution remained liquid in a glass bottle at 37 °C and could not be cured even after UV light activation (Fig. S1). In addition, it was confirmed that Gelatin and GelNB was hydrolyzed by digestive enzymes at normal temperature and was digestive enzyme-resistant at low temperatures by incubating Gelatin and GelNB in the simulated intestinal fluid at 4 °C and 20 °C for 2 days (Fig. S2), and the fluorescently labeled GelNB which was allowed to adhere to aminated plates incubate with the simulated intestinal fluid for 24 h at 37 °C was observed under a fluorescent microscope (Fig. S3). These findings indicate that most of the –NH₂ on the chain of the Gelatin molecules was replaced by NB. This ensured that there were enough photo-generated aldehyde groups on GelNB, which could later bond with –NH₂ on the surface of the intestinal lumen tissue and was fixed to form a thin molecular coating as a physical barrier. Moreover, the highly dynamic activated GelNB solution could also ensure better uniform administration, avoiding the quick discharge due to inadaptation to intestinal peristalsis when applying the traditional hydrogels [22].

IBD often presents with acute attacks under stress. In this case, therapeutic materials that perform treatment functions faster, more stable, and longer sustainability will have significant application prospects [27]. To ensure a similar satisfactory adhesion and retention of the biophysical barrier in the intestinal epithelium, we investigated the formation of the molecular coating on the intestinal surface by confocal microscopy through focusing (CMTF). Fig. 2A showed that the fluorescently labeled GelNB was able to stick to the intestinal wall and form a thin but dense coating on the scale of hundreds of nanometers. The fluorescence intensity of the Gelatin group was very weak, similar to that of the control group, indicating that Gelatin failed to firmly adhere to the intestinal wall. *In vitro* experiments showed that both Gelatin and GelNB were able to adhere to the aminated plates (Fig. 2B) at the beginning of the experiment; however, only GelNB maintained initial adhesion levels after repeated washing with PBS for 24 h at 37 °C. These results demonstrate that GelNB could form a uniform and stable coating on the surface of the intestine.

Scanning electron microscopy (SEM) was used to further investigate the GelNB molecular coating on the intestinal surface. As shown in Fig. 2C, the normal colon was consisted of a single layer of columnar epithelium, covered with tiny protuberations. While the changes were not obvious in the Gelatin-treated group, the GelNB-treated group showed a dense coating, indicating that GelNB strongly adhered to the colonic surface and formed a physical protective barrier on the mucosal
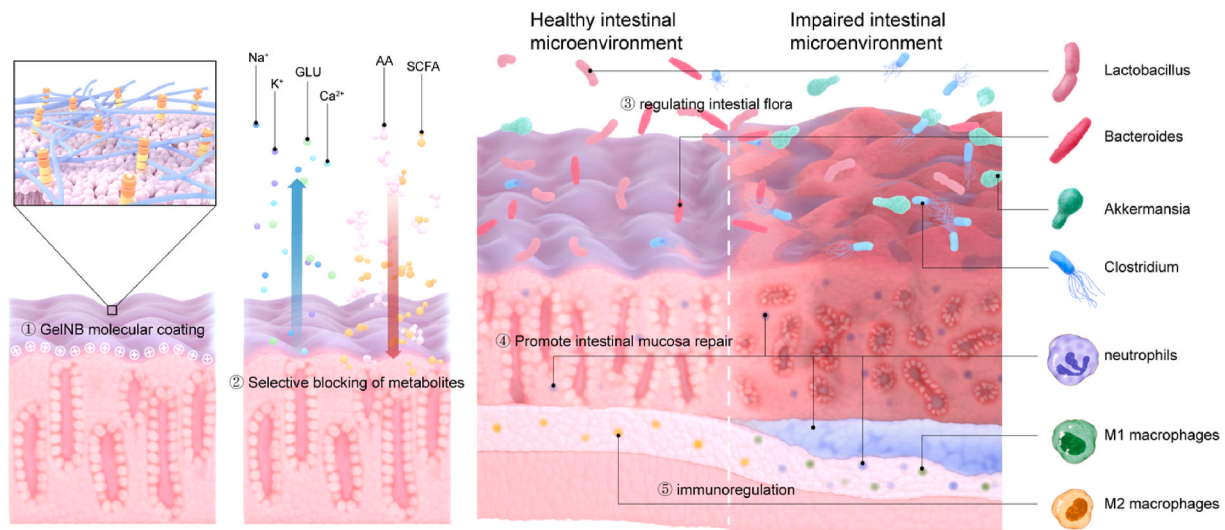
Fig. 1. GelNB molecular coating acts as biophysical barrier to isolate intestinal metabolites irritations and regulate intestinal microbial homeostasis.

surface.

IBD patients have a certain degree of intestinal nutrition metabolism disorder. Thus, inappropriate diets, such as high fat intake diet (HFD) [28], high protein intake diet (HPD) [29], and high carbohydrate diet (HCD) [30], are considered as risk factors for IBD, which may further induce intestinal inflammation by disturbing the metabolism of intestinal epithelium, converting intestinal flora, and aggravating the instability of the intestinal environment through continuous inflammation [31]. Therefore, there is a need to verify whether the GelNB molecular coating has the ability to function as a physical barrier. Intestinal mucosal damage and inflammation caused by IBD can cause electrolyte secretion and absorption disorders, especially with regards to Ca^{2+}, Na^+, K^+, and other ions, resulting in acid-base imbalance [32]. We hypothesized that if this layer of glue has a physical barrier function, the contents of the external physical stimuli would not be able to pass through the intestinal tract. To verify physical barrier function of GelNB *in vitro*, we applied GelNB on dialysis bag as to simulate its application on the surface of the intestinal surface, which could be directly acquired by the different concentrations inside and outside the dialysis bag. Fig. 2D showed that the infiltration of glucose in the GelNB-treated dialysis bags was significantly inhibited within half an hour compared to that in the Gelatin-treated dialysis bags, with an inhibition that lasted for 2 h ($P < 0.01$). It has been reported that high glucose instigates macrophages and other immune cells in the direction of proinflammation [33]. Therefore, the low osmotic effect of GelNB on glucose may have an impact on the intestinal immune response. Free fatty acids (NEFA), such as butyrate, are small molecular compounds produced by intestinal microbes that decompose dietary fiber. GelNB significantly promoted the penetration of NEFAs ($P < 0.05$) (Fig. 2E). Butyrate has been reported to regulate Treg production and enhance the activity of macrophages to prevent colitis [34]. Amino acid uptake is also closely related to the progression of IBD [35]. In this context, we selected four kinds of amino acids for the osmotic experiment, among which glutamine, glutamate, and glycine were found to easily permeate into the dialysis bag through GelNB in the intestinal environment ($P < 0.05$) (Fig. 2F). Studies have shown that glutamine can increase the expression of tight connexin and promote intestinal repair [36], while glycine can reduce MPO activity in colon tissue [37], and can reduce the expression of vascular endothelial growth factor (VEGF-A) and its receptor, inhibiting the increase in vascular density caused by inflammation, and reducing the aggregation of intestinal granulocytes [38]. This suggested that the selective absorption of amino acids by GelNB may contribute to the recovery of IBD. In addition, Fig. 2G showed that GelNB could prevent the exchange of electrolyte in the intestinal tract, as the positive

ions (e.g. Ca^{2+}, Na^+, and K^+) in the dialysis bag appeared to be higher in Gelatin than in GelNB ($P < 0.05$).

Ca^{2+}, Na^+, K^+, and arginine were all positively charged and were blocked by GelNB, while glutamine, glutamate, and glycine were negatively charged and tended to be absorbed by the intestine covered with GelNB (Fig. S4). Thus, we speculated that the GelNB molecular coating might selectively absorb nutrient substances, thereby reducing the irritation of nutrients to the gut. In order to further explore the mechanism by which GelNB selectively permeates metabolites in the intestinal lumen, we measured the zeta potential on the surface of GelNB. We found that the zeta potential on the surface of GelNB was 6.91 mV (Fig. S5), suggesting that GelNB might act as a physical barrier, represented by a charge barrier, to affect substance exchange.

The above results demonstrated that GelNB could form a stable, dense, highly adhesive, and biocompatible molecular coating on the intestinal epithelium, which served as an ideal *in vitro* physical barrier. Previous studies have suggested that the occurrence and development of IBD is closely associated with inflammatory factor infiltration, microbial invasion, intestinal metabolic substances, and other stimulating factors in the intestinal environment [4,25]. The physical barrier function of GelNB could segregate the stimulating factors to a certain degree, thereby reducing inflammatory infiltration.

2.2. In vitro study on the properties of GelNB molecular coating to promote regeneration and inhibit inflammation

Failure of mucosal healing (MH) is a characteristic manifestation of IBD. Therefore, mucosal healing (MH) is considered an important therapeutic goal and a key indicator for determining the prognosis of IBD patients [39]. One of the most crucial characteristics for evaluating biomaterials is their ability to promote regeneration, namely the proliferation and migration of epithelial cells [40]. In contrast to immune cells and fibroblasts, epithelial cell migration is carried out to form an aggregated lamellar structure, which is directional and depends on the polar distribution of the cells and the remodeling of the cytoskeleton [41]. In this context, we performed several *in vitro* experiments to evaluate the function of GelNB in promoting mucosal healing from several perspectives.

To investigate the effect of GelNB on the proliferation of damaged epithelium, we performed live/dead staining and CCK-8 colorimetry *in vitro*. As shown in Fig. 3A, live/dead staining of the intestinal epithelial cells showed that the number of live cells in the GelNB group was significantly higher than that in the other two groups after three days of culture. Similar results were obtained for CCK-8, and the cell
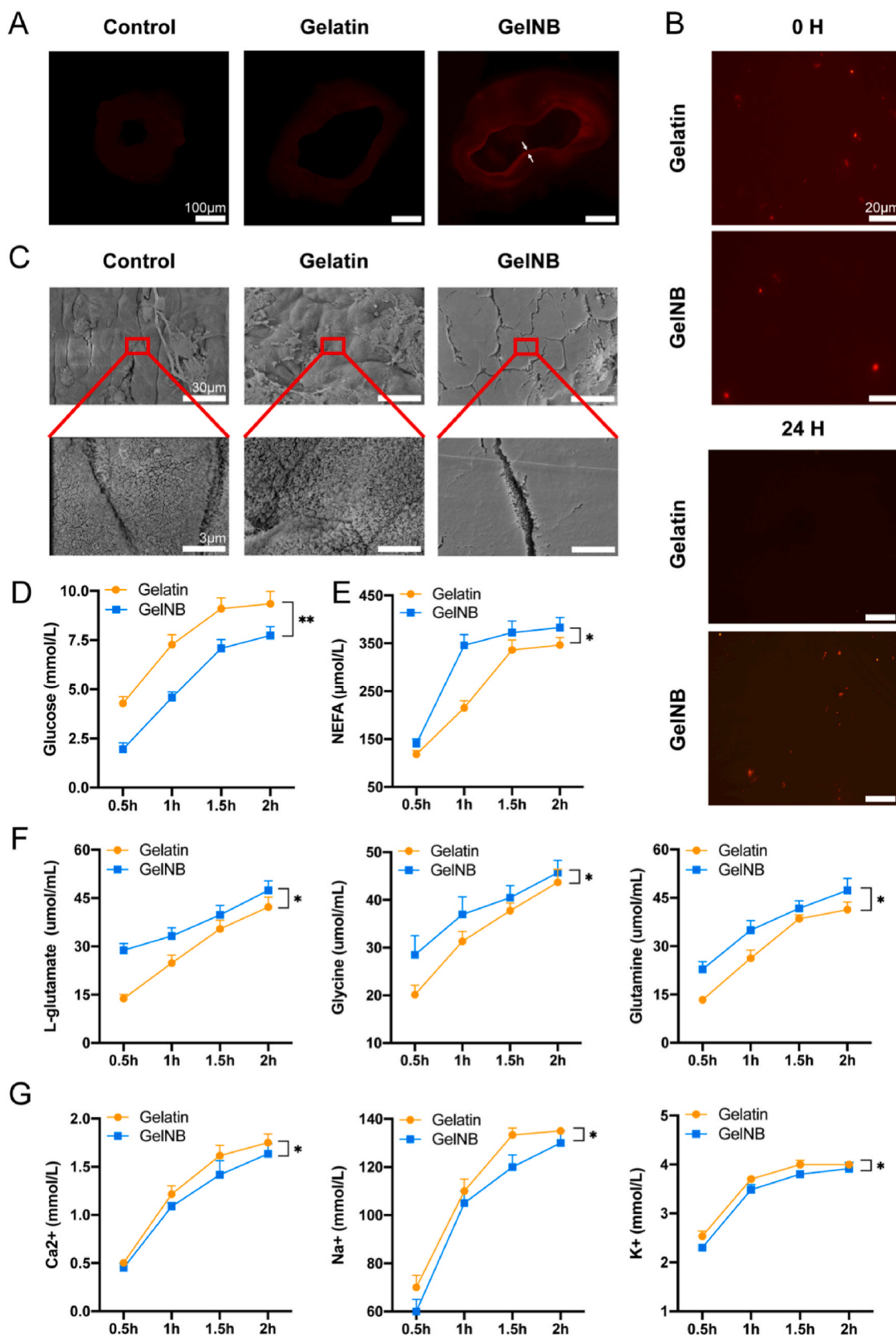
Fig. 2. Characterization of *in vitro* adhesive performance and physical barrier function of GelNB molecular coating.
(A) Fluorescence images of mice colonic surface labeled by Gelatin and GelNB molecular coating (scale bars: 200 μm). **(B)** Fluorescence images of labeled Gelatin- and GelNB molecular coating-treated aminified plates at 0 h and 24 h (scale bars: 20 μm). **(C)** SEM images of colonic surface in non-treated group and treated by Gelatin and GelNB molecular coating respectively (scale bars: 30 μm (top panels); 3 μm (bottom panels, enlarged)). **(D–G)** Measurement of glucose(D), NEFA(E), amino acid (F), and ion (G) absorption by using the Gelatin-and GelNB molecular coating-pretreated dialysis bag. (*p < 0.05 and **p < 0.01).
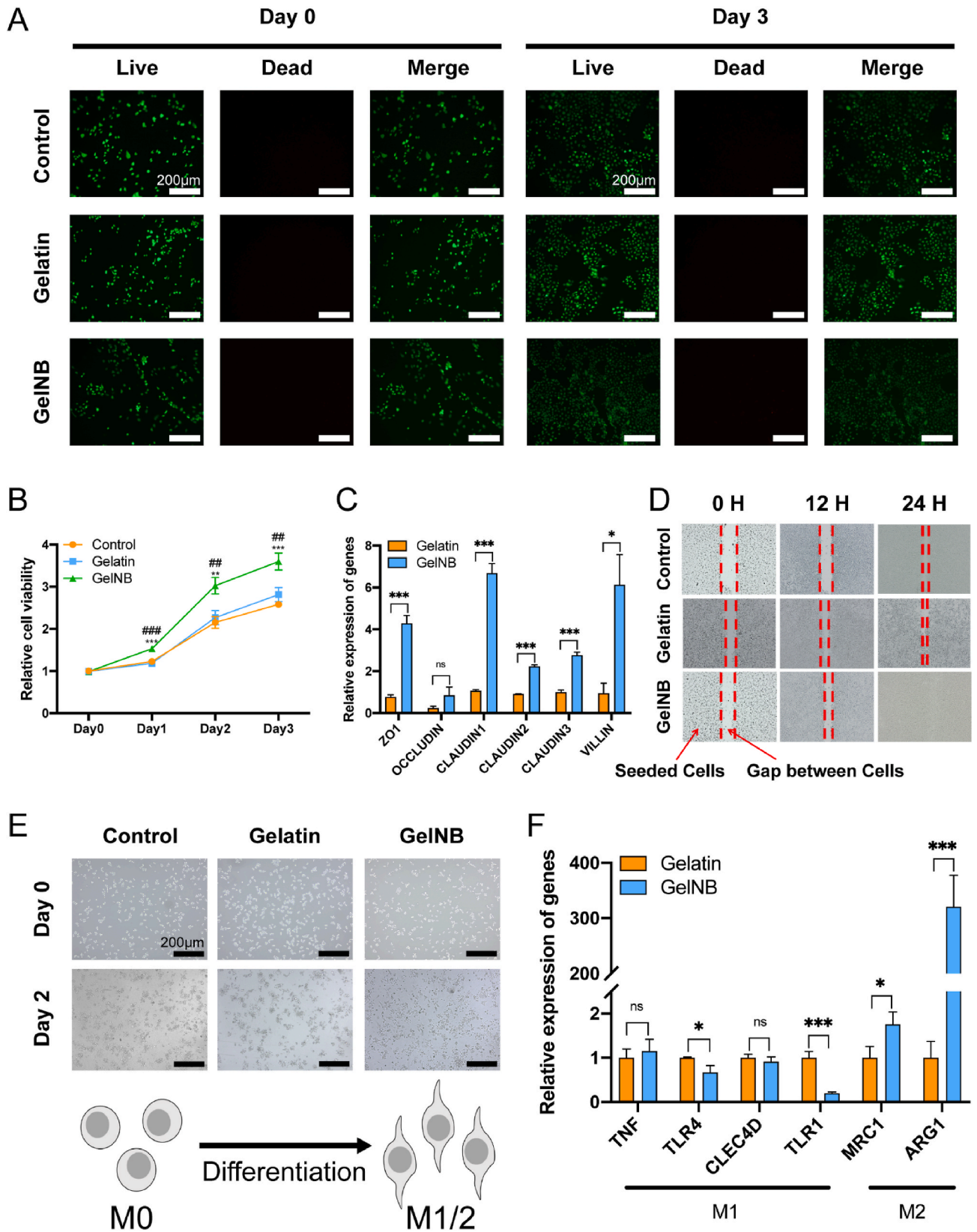
Fig. 3. *In vitro* mucosal repair and regeneration of GelNB molecular coating.
(A) Live/Dead staining of NCM460 cells loaded Gelatin and GelNB molecular coating at Day 0 and Day 3. **(B)** Detection of CCK-8 to quantify cell viability in NCM460 cells culture at different time points in control, Gelatin and GelNB groups. **(C)** qPCR analysis of the expression differentiation in genes related to physical intestinal barrier function. **(D)** Wound healing ability of NCM460 cells in plates pretreated by negative control, Gelatin and GelNB molecular coating (scale bars: 200 μm). **(E)** Morphological changes after culturing macrophages *in vitro* Gelatin and GelNB molecular coating. **(F)** GelNB induced macrophages to differentiate into M2 instead of M1 in mRNA expression level.

proliferation capacity of the GelNB group was significantly higher than that of the Gelatin and NC groups on day 3 ($P < 0.001$) (Fig. 3B). Both experiments showed that GelNB molecular coating can dramatically promote the proliferation of intestinal epithelial cells, which is beneficial for intestinal repair.

IBD is often accompanied by the destruction of the intestinal mucosal structure and an increase in intestinal mucosal permeability. As the structural basis of mucosal healing, cytoskeleton remodeling can restore and maintain the complete barrier function of the intestinal epithelium, wherein tight junction-related proteins ZO-1, Occludin-1, and Claudins are the key regulatory factors of the cytoskeleton [42]. These results revealed that GelNB could significantly increase the expression of *ZO-1*
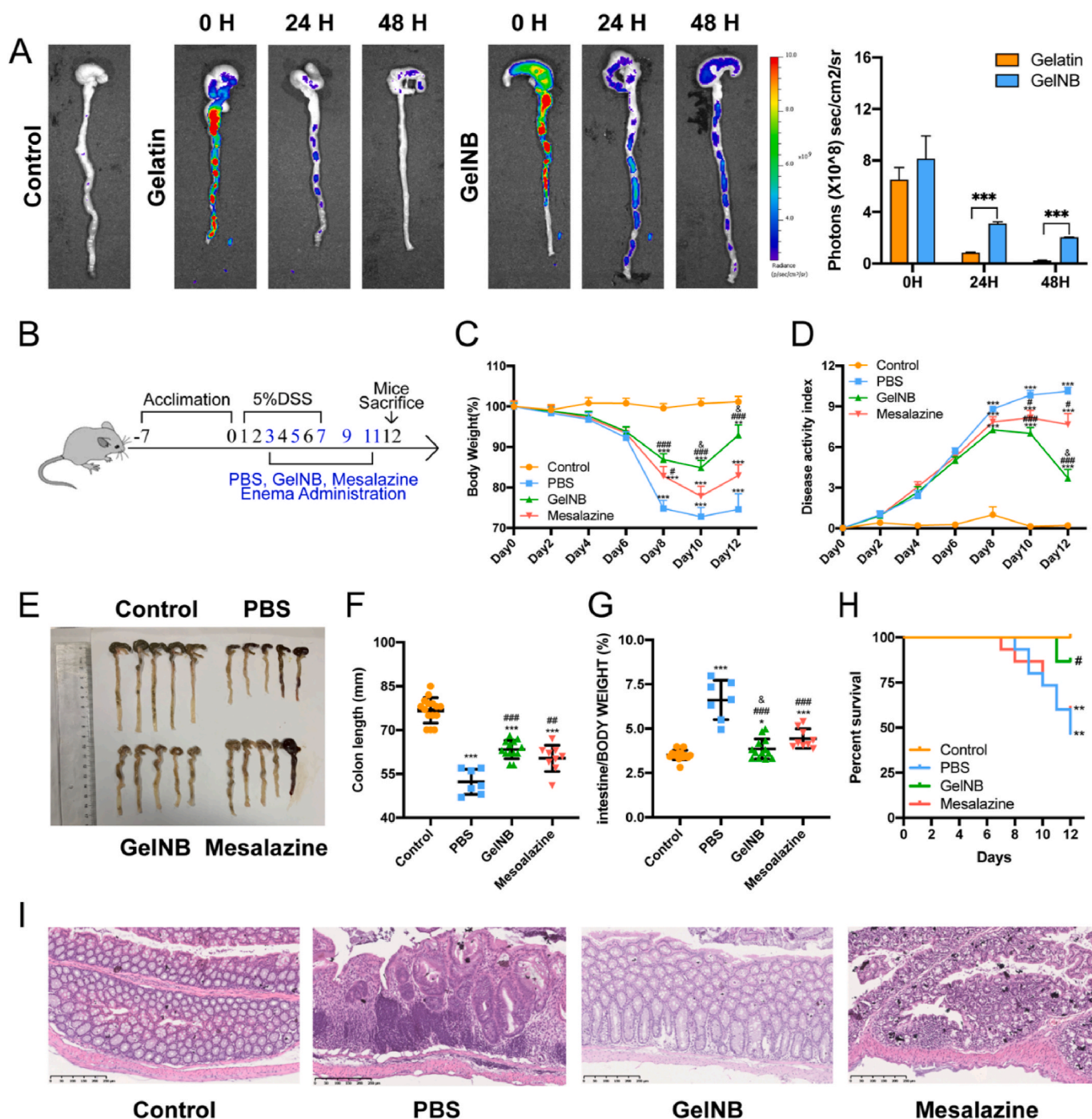

Fig. 4. *In vivo* GelNB molecular coating promotes the recovery of IBD in DSS-induced mice.
(A) Fluorescence was detected using IVIS Spectrum to compare the colonic retention time of labeled Gelatin and GelNB molecular coating in mice. **(B)** The schema of the DSS-induced mice and the treatment process in three groups. **(C)** Percentage of body weight loss after the treatment of negative control, Gelatin and GelNB. **(D)** The measurement of DAI score after treatment. The weight loss index, bloody stool index, and stool consistency index were calculated. **(E)** Macroscopic images of colonic tissues at Day 12 after treatment. **(F)** Quantitative colon length after 12-days of different treatments. **(G)** Quantitative ratio of the colon weight to mice body weight after treatment. **(H)** The survival curves in each group of mice treated by negative control, Gelatin and GelNB. **(I)** Representative histological sections of colons by H&E staining (scale bar: 50 μm). Data are expressed as the mean ± SEM. n = 15. *p < 0.05, ***p < 0.001 versus Control; #p < 0.05, ##p < 0.01, ###p < 0.001 versus PBS; &p < 0.05 versus Mesalazine.

and *Claudins* at the mRNA level ($P < 0.001$) (Fig. 3C), indicating that GelNB functioned to strengthen the intestinal barrier integrity and promote mucosal healing.

In addition, the healing of defective epithelium can only be repaired more rapidly when a given biomaterial recruits surrounding epithelial cells [21]. Therefore, we tested whether GelNB could promote this migration using a cell scratch experiment. After the GelNB was applied on the surface of the culture dishes, the migration rate of cells was significantly faster than that of the control group and the Gelatin treatment group at 12 h, and almost covered the scratch area within 24 h (Fig. 3D). This suggested that the GelNB molecular coating enhanced cell migration and aggregation to recruit surrounding cells for the repair of damaged epithelium.

Macrophages are one of the major effector cells that regulate tissue repair in IBD. The phenotypic changes in macrophages are mediated by the inflammatory environment and immune microenvironment at the injured site. M1-differentiated macrophages can release inflammatory cytokines to induce an inflammatory response, while M2-differentiated macrophages secrete interleukin-10 (IL-10) to alleviate inflammation. Therefore, altering the balance from the M1 to M2 macrophage phenotype is a critical factor influencing the inflammatory outcome of IBD [43–45]. We cultured macrophages on GelNB-and Gelatin-coated dishes and found that GelNB coating significantly promoted the expression of *MRC1* ($P < 0.05$) and *ARG1* ($P < 0.001$), which characterized the differentiation of macrophages M2 (Fig. 3E and F), while the expression of *TLR1* ($P < 0.001$), *TLR4* ($P < 0.05$), and other genes that characterized macrophage M1 differentiation were significantly inhibited. Meanwhile, the expression of *CLEC4D* in the GelNB group also showed a downward trend. These results indicated that, compared with Gelatin, GelNB could further promote the phenotypic transformation of macrophages toward M2-polarization, tilting the balance toward M2-type, and alleviating the inflammatory response.

2.3. GelNB molecular coating promotes the recovery of DSS-induced colitis in IBD mice

After confirming that GelNB had a reliable function as a mucosal barrier and is capable of promoting the healing process, *in vitro* imaging technology was used to observe the distribution and retention time of stained GelNB in the intestine at 0, 24, and 48 h to determine the therapeutic effect and potential mechanism of GelNB molecular coating on IBD at the tissue level. Fig. 4A showed that GelNB remained more adhesive in the colon of the mice at 48 h. By contrast, the mice treated with Gelatin showed only faint fluorescence in the colon, most of which had already been expelled. This illustrated that GelNB had better retention performance, which was the basis for our subsequent application in mice.

With the westernization of diets, the incidence of UC is increasing annually. Patients with mild UC have less than four diarrheas per day. However, once they progress to severe UC, these symptoms come with an acute onset, including diarrhea, blood in the stool, and persistent severe abdominal pain, and can sometimes accompanied by hypotension and shock. Thus, early intervention to prevent further deterioration is an urgent clinical problem that needs to be addressed. We established DSS-induced mice with IBD as a model, performed different interventions, and evaluated the effects of treatment. The UC model is characterized by increased epithelial damage and the production of large numbers of inflammatory cytokines [46,47]. Mesalazine is widely used as a basic treatment for IBD in clinical practice [48]. In order to demonstrate the prophylactic and therapeutic effects of GelNB molecular coating on the DSS-induced IBD model, we set the PBS-treated group and mesalazine-treated group as the control.

According to previous studies, DSS generally takes 7–9 days to induce acute UC in mice. The first one to three days represent the initial stage of inflammatory injury, during which the clinical symptoms and pathological changes of the colon in mice are usually not obvious [49].

To evaluate whether GelNB had a preventive effect on IBD progression, we administered PBS, GelNB, and mesalazine to mice by enema on day 3 after mice received DSS-drinking water. In order to exclude the potential influence of GelNB or PBS treatment on DSS modeling, we explored the influence of GelNB or PBS treatment on drinking water and diet in mice, and confirmed that no significant difference existed between the two groups (Fig. S6). Considering that GelNB maintained relatively high adhesion at 48 h, to reduce the damage caused by enema in mice, we administered GelNB every 48 h. After continuous administration to day 11 (Fig. 4B), the body weight of mice in the PBS group continued to decrease, with a decrease rate of approximately 20% on day 8, and the decrease in the other two groups was less than that in the PBS group ($P < 0.001$) (Fig. 4C). This indicated that both GelNB and mesalazine had a protective effect on weight loss induced by DSS in IBD mice. Surprisingly, weight loss in the GelNB group was less than that in the mesalazine group before day 8 and showed a significant weight recovery after day 8, indicating that as the pathogenic factors continued to severe, GelNB could prevent weight loss.

We also continuously measured the disease activity score (DAI) to evaluate the severity of colitis. The score of the GelNB-treated group began to decrease after day 8. It is worth noting that the median DAI score of day 12 mice was restored to 4 (Fig. 4D), with a remarkable downward trend. According to the weight of GelNB group mice on day 12, the score corresponding to "weight loss" in DAI was 2. Interestingly, based on the weight recovery trend on day 8–12, we assumed that the weight of the mice remained in a significant upward trend at day 12, and the weight of the GelNB group mice would further recover until it was close to the value of the control group. Furthermore, the DAI of the GelNB group mice would also have a sustained reduction to close to or equal to the value of the control group. This result also suggested that treatment with GelNB in the early stage of IBD rapidly slowed down the trend of the disease's development into severe disease, quickly restoring it to normal levels.

The ratio of colon weight to length is an indicator of inflammatory edema [50]. After euthanasia on day 12, we performed a general examination of the intestines and found that GelNB reversed the pathological shortening of colon length caused by colitis, and the colonic morphology of GelNB group mice was also closest to that of normal control group mice when compared to other treatments (Fig. 4E, F, and 4G). As severe UC has a certain mortality rate, when the experiment lasted until day 12, the survival rate of the GelNB-treated group was as high as 90%, while that of the PBS-treated group and mesalazine-treated group decreased to 50% and 60%, respectively (Fig. 4H).

In addition, histological examination based on hematoxylin-eosin (H&E) staining showed typical histopathological features of colitis in the PBS group, including severe epithelial ulceration, loss of cup cells, and excessive infiltration of intraepithelial lymphocytes. In contrast, the GelNB- and mesalazine-treated groups had less mucosal inflammation, less colonic congestion, and edema. However, the histological manifestations of the GelNB-treated group were more similar to those of the normal control group (Fig. 4I) compared to the mesalazine-treated group. Moreover, the colonic damage score of the GelNB group also showed that the degree of inflammation, the depth of inflammation, and the degree of gland damage were lower than those of the other groups (Fig. S7). These results indicated that the GelNB molecular coating could inhibit the progression of UC. GelNB molecular coating could also reduce the mortality of severe cases by restoring the weight of mice and improving intestinal inflammation, which is of great guiding significance in clinical practice.

2.4. GelNB molecular coating acts as a molecular barrier and modulates the immune response in vivo

For the treatment of IBD, the inhibition of the inflammatory status is one of the strategic points to evaluate the efficacy of novel biomaterials. Increased reactive oxygen species (ROS) have been reported to

contribute to the development of colitis [51]. We evaluated the level of ROS in mice using bioluminescence imaging (BLI) [52]. On day 3, the level of ROS was found to remain essentially the same, while on day 12, the ROS detection was five times higher in the PBS-treated group than in other groups, with the GelNB-treated group presenting less ROS than the mesalazine-treated group. This indicated that GelNB molecular coating could significantly decrease the level of ROS ($P < 0.001$) (Fig. 5A and B). In addition, to explore whether GelNB could act as a physical barrier to regulate the inflammatory response, we also evaluated the expression difference of myeloperoxidase (MPO) among the groups. MPO is a heme protein rich in neutrophils, synthesized in the bone marrow by granulocytes before entering the circulation and stored in phagocytic granules. External inflammatory stimuli can lead to the accumulation of neutrophils, thereby releasing MPO. MPO staining (Fig. 5C) showed that a large number of neutrophils infiltrated the intestinal epithelial sections of both mesalamine and PBS groups, while the number of neutrophils in the GelNB-treated group was closer to that in the normal group. Similarly, the MPO expression level was measured using the MPO assay kit, and it was confirmed that after DSS treatment, MPO activity in PBS-treated mice and mesalazine-treated mice was maintained at a high level in comparison with GelNB-treated mice (Fig. S8). The working mechanism of mesalazine in the clinical treatment of IBD involves the inhibition of the NF-κB pathway, the regulation of the PPARγ receptor, and the inhibition of the expression of inflammatory factors, such as TNFα, IL-1, and IL-6. As shown in Fig. 5D, the expression of pro-inflammatory factors, such as IF-1α ($P < 0.05$), IF-1β ($P < 0.001$), IL-6 ($P < 0.05$), TNF-α, iNOS, and IFN-γ in the tissues after treatment with GelNB were significantly decreased compared with the mesalazine group, while the expression of anti-inflammatory factors, such as IL-4 and IL-10, was increased. This suggested that the better effect of GelNB than mesalazine may be due to its stronger inhibition of the local inflammatory response.

In addition to regulating the immune response, we also investigated the regenerative function of GelNB molecular coating on the intestinal epithelial cell barrier. We analyzed the degree of cell proliferation at the tissue level by detecting the expression of Ki-67 in the intestinal tract of mice via immunohistochemical staining. Compared with the GelNB and mesalazine groups, the PBS group had fewer Ki-67-positive cells, indicating that the ability to improve the proliferation of intestinal columnar epithelial cells was significantly enhanced in GelNB and mesalazine compared with PBS (Fig. 5E and Fig. S10).

The intestinal epithelial tight junction (TJ) is a pivotal structural basis for the function of the intestinal barrier, and the damage to TJs leads to increased intestinal permeability. The early onset of IBD is often accompanied by increased intestinal mucosal barrier permeability [53], resulting in changes in proteins (ZO-1 and Occludin-1), which represent the expression of TJs [54]. We detected the expression of ZO-1 and Occludin-1 using immunohistochemical staining. As shown in Fig. 5E, IBD could destroy the intestinal mucosal barrier, resulting in decreased ZO-1 and Occludin-1 expression, indicating that the TJs between cells were destroyed and the permeability of the intestinal epithelium was elevated. However, after enema administration of GelNB, the damage to TJs was reversed, prompting the expression of Occludin-1 and ZO-1 to return to normal levels; comparatively, the effects of mesalazine were less evident (Figs. S9A and S9B). Moreover, the histopathological images of major organs including lung, spleen, kidney, liver and heart showed that no significant differences were observed among the different groups implying the good biocompatibility of the GelNB (Fig. S11).

These results fully demonstrated that GelNB molecular coating could stabilize the mucosal barrier in the early stage of IBD and prevent the further destruction of the mucosal barrier over time. On the one hand, under the action of GelNB molecular coating, the expression levels of the TJ proteins ZO-1 and Occludin-1 increased, resulting in the timely repair of the TJs of damaged intestinal epithelial cells, thus maintaining a strong barrier function to prevent further stimulation of intestinal epithelium by DSS. On the other hand, neutrophil infiltration in IBD was inhibited by GelNB molecular coating, thus maintaining the immune homeostasis of the environment, providing a favorable environment for barrier repair and the prevention of DSS stimulation.

2.5. Therapeutic effect of GelNB molecular coating on TNBS-induced IBD mice

After exploring the preventive and protective effects of GelNB molecular coating on IBD, we further explored its therapeutic effect. CD, another subtype of IBD, also widely affects the global population, particularly in East Asia and South America [55]. We used the TNBS model to simulate CD [56] to test whether GelNB had the same therapeutic effect. The mechanism of TNBS-induced IBD involves the use of ethanol as a destructive agent of the intestinal mucosal barrier and enables TNBS to bind to the perfect antigen of intestinal mucosal keratin, stimulating the local immune response [57]. We began treatment on day 2 and, similar to DSS, administered PBS, GelNB, and mesalazine enemas every other day (Fig. 6A) to observe whether GelNB molecular coating could prevent the progression of severe IBD and delay weight loss.

We chose continuous observation for one week after TNBS induction as the time window for evaluation as studies have shown that injury can completely disappear on day 7 after TNBS, making it difficult to compare efficacy among groups [58]. As such, an observation time of seven days was considered to be optimal. Five days before the experiment (Fig. 6B), the weight of mice in the three groups continued to decrease; however, the weights of the GelNB-treated group mice were always the highest among the three groups. Moreover, after TNBS effect for three days, the weight of the PBS-treated group and mesalazine-treated group continued to decline, while the weight of the GelNB-treated group tended to be stable and presented an upward trend, which suggested that GelNB molecular coating could delay the progression of CD to severe illness. Correspondingly, while the DAI scores decreased in both the GelNB- and mesalazine-treated groups, the prophylactic effect of GelNB was higher than that of mesalazine (Fig. 6C). After euthanasia on day 7, the intestinal gross examination results of TNBS-induced mice were similar to those of DSS-induced mice. GelNB molecular coating could also reverse the pathological shortening of colonic length caused by colitis, and restore the colon/body weight to nearly normal levels (Fig. 6D, E, and F). The colonic damage score also proved that GelNB treatment could significantly cure TNBS-induced IBD ($P < 0.001$), and the therapeutic effect was significantly better than that of mesalazine ($P < 0.001$) (Fig. S12). In terms of microstructure, histological examination of H&E staining showed that the intestinal epithelial ulcers in the PBS group were more severely damaged and had a larger number of inflammatory cell infiltrations, while the intestinal epithelial edemas in the GelNB group were less severe and the histological manifestations were the closest to normal (Fig. 6G).

Similarly, we investigated whether GelNB molecular coating also served as a physical barrier in regulating the inflammatory response in TNBS-induced IBD. The fluorescence imaging results showed that on day 12, the fluorescence intensity of ROS in the abdominal cavity of GelNB-treated mice was significantly lower than that of the PBS-treated group and mesalazine-treated group, indicating that the inflammation level of mice treated with GelNB for 12 days essentially declined to normal levels (Fig. 6H and I). We also measured the expression levels of a series of pro-inflammatory factors using qPCR. Immunohistochemical staining of the proliferation index (Ki-67) and intestinal barrier index (ZO-1 and Occludin-1) also showed an effect similar to that of the DSS group (Fig. 6J, Figs. S13A and S13B, Fig. S15). Finally, we used quantitative real-time PCR (qPCR) to determine the expression levels of a series of pro-inflammatory factors. As shown in Fig. S14, the results showed that GelNB treatment significantly reduced the expression of IL-1α, IL-1β, IL-6, TNF-α, iNOS, and IFN-γ. In contrast, mesalazine treatment could only alleviate the high-level expression of pro-inflammatory factors.
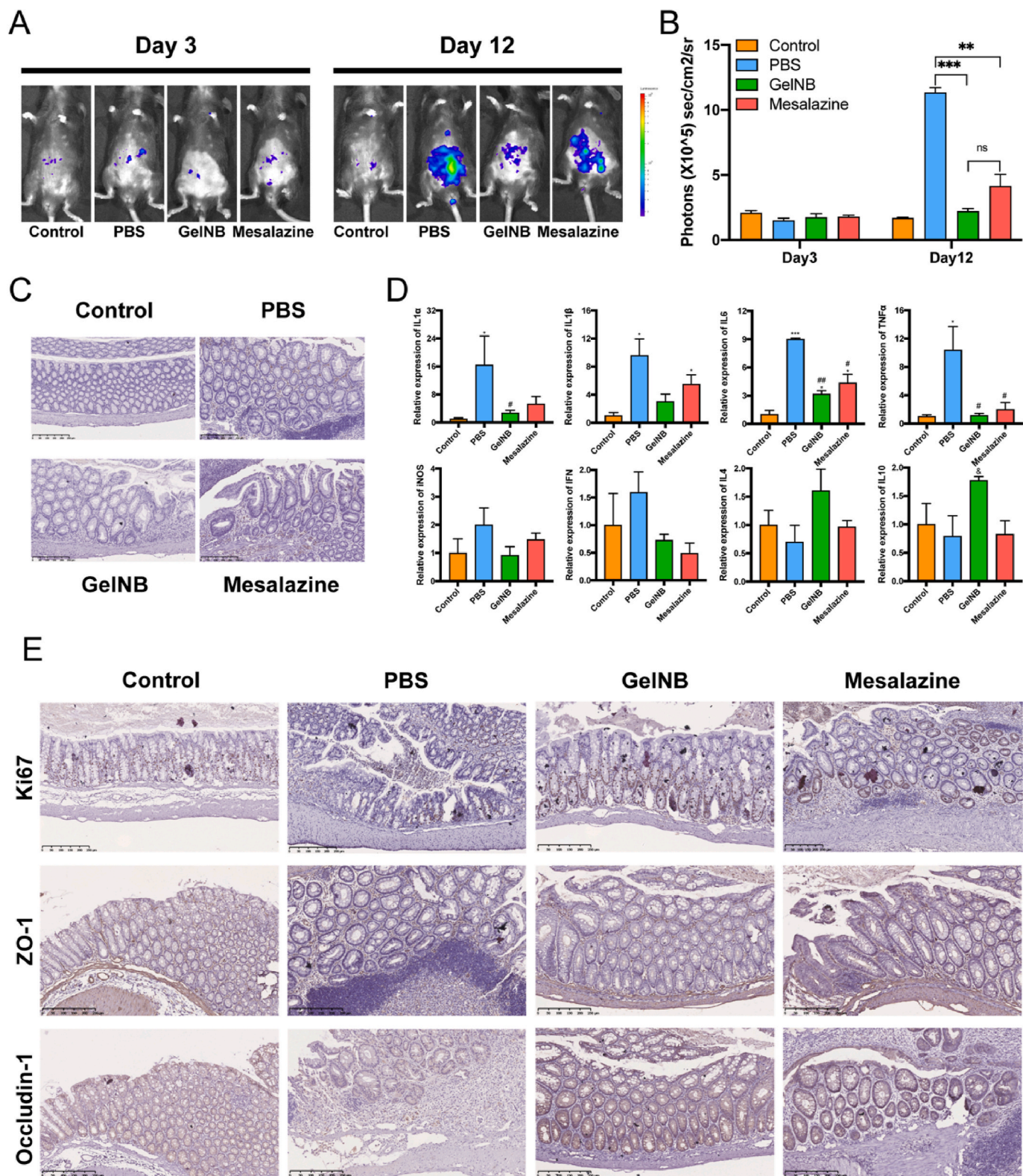
Fig. 5. *In vivo* the molecular barrier function and immunoregulatory capability of GelNB molecular coating in DSS-induced model.
(A) ROS activities were more active in PBS, Gelatin and Mesalazine group in comparison with mice in GelNB group. **(B)** Quantitative analysis of ROS signals. Data were expressed as the mean ± SEM. **p < 0.01, ***p < 0.001. **(C)** Representative images of immunohistochemical staining of MPO (scale bar: 50 μm). **(D)** qPCR analysis of the distal colon for intestinal inflammation-related genes. Data were expressed as the mean ± SEM. *p < 0.05, ***p < 0.001 versus Control; #p < 0.05, ##p < 0.01 versus PBS; &P < 0.05 versus Mesalazine. **(E)** Representative Ki-67, ZO-1, and Occludin-1 immunohistochemical staining in tissue sections (scale bar: 50 μm).
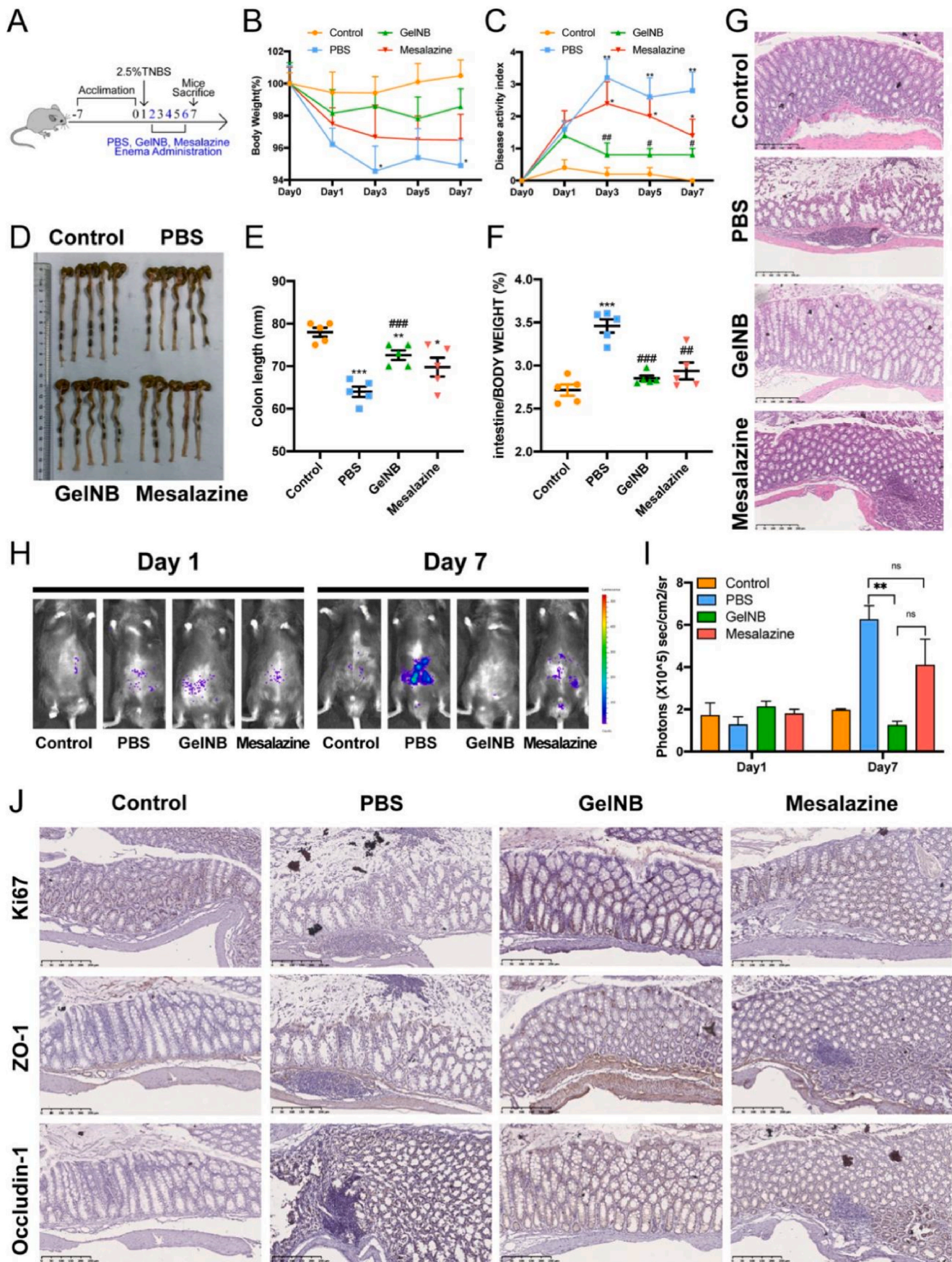
(caption on next page)

Fig. 6. *In vivo* GelNB molecular coating promotes the recovery of TNBS-induced mice.
(A) The schema of the TNBS-induced mice for four different treatment. **(B)** Percentage of body weight loss after the treatment of negative control, Gelatin, Mesalazine and GelNB. **(C)** The DAI score after treatment, which included the weight loss index, bloody stool index, and stool consistency index. **(D)** Macroscopic images of colonic tissues at Day 7 after the initial treatment. **(E)** Quantitative colon lengths were measured and compared between groups. **(F)** Quantitative ratio of the colon weight to mice body weight in TNBS model. **(G)** Representative histological sections of mice colons stained with H&E (scale bar: 50 μm). **(H)** and **(I)** Images of ROS activities and Quantitative analysis of ROS signals in mice colitis. **(J)** Representative expresion of Ki-67, ZO-1, and Occludin-1 in colon sections by immunohisto-chemistry staining (scale bar: 50 μm). Data are expressed as the mean ± SEM. n = 5. *$p < 0.05$, **$p < 0.01$, ***$p < 0.001$ versus Control; #$p < 0.05$, ##$p < 0.01$, ###$p < 0.001$ versus PBS.

2.6. GelNB molecular coating acts as a biological barrier by regulating intestinal flora

We verified the prophylactic and therapeutic effects of the GelNB molecular coating on IBD *in vitro* and *in vivo*, and proved that GelNB molecular coating can act as a physical barrier to achieve a protective effect against IBD. Moreover, evidence increasingly supports the idea that intestinal flora are deeply involved in the pathogenesis of IBD, and changes in intestinal barrier function and inflammatory environment can also influence the composition of intestinal flora [59]. The major changes in IBD are the reduction of bacterial diversity and the absence of anaerobic bacteria, which drive the flora environment to shift in the pro-inflammatory direction [60,61]. Here, we continued to study the microbial regulation mechanism of GelNB molecular coating on IBD, and explored whether GelNB molecular coating could play a biological barrier role in regulating intestinal microbes. To this end, the feces of the experimental animals were collected and analyzed by 16S rDNA sequencing to compare the diversity and transformation of intestinal flora in each group.

First, principal component analysis (PCoA) was used to evaluate the similarity among the samples. The shorter the distance between the points in each sample, the closer the expression trend of genes, which could also be interpreted as smaller differences among the samples. On the basis of the good uniformity of data in each group, we found that the distance between the normal control group and GelNB group was the smallest, followed by the mesalazine-treated and PBS-treated groups. This indicated that the GelNB molecular coating promoted the recovery of intestinal flora, which was closer to the normal intestinal flora. The ability of the GelNB molecular coating to regulate intestinal flora was stronger than that of mesalazine (Fig. 7A). PCoA and the results of non-metric multidimensional scaling (NMDS) (Figs. S16A and S16B) also supported this conclusion.

At the genus level, we further found that *Muribaculaceae* (48.63%) and *Lactobacillus* (7.32%) were the dominant bacteria at the genus level in the intestinal tract of normal control group mice (Fig. 7B). After inducing IBD, the relative abundances of these two types of microorganisms decreased significantly. At the same time, the relative abundance of *Ruminococcaceae_UCG-014* (26.49%) and *Akkermansia* (20.06%) increased sharply. We found that at the genus level, the normal flora structure was also the most similar to that of the GelNB-treated group, among which *Muribaculaceae* and *Ruminococcaceae_UCG*-014 had the most significant recovery of abundance. We also found that GelNB molecular coating greatly recovered the proportion of *Lactobacillus* (24.27%), which may be due to the GelNB molecular coating inhibiting DSS to induce lactic acid bacteria [62]. Through further cluster analysis, we found that the flora structure of the GelNB-treated group was most similar to that of the normal control group at the level of class, order, family, and species (Figs. S17A, S17B, and S17C, respectively). These results suggested that GelNB molecular coating had a positive regulatory effect on the intestinal flora.

As shown in the heat map in Fig. 7C, the flora structure of the GelNB-treated group was closest to that of the normal control group. As the main phylum in the intestinal flora, during the progression of IBD, the abundance of beneficial *Bacteroidetes* and *Firmicutes* would significantly decrease in the intestinal environment of IBD, while the abundance of harmful *Verrucomicrobia* would significantly increase [63,64], which was confirmed by our heat map results. The results indicated that GelNB

treatment restored the abundance of the two beneficial bacteria to normal levels in the control group. At the order and family level, GelNB molecular coating was also found to inhibit the abundance of harmful bacteria, while restoring the decrease in abundance of beneficial bacteria caused by IBD at the same time (Figs. S18A and S18B).

To further examine the dominant flora and regulatory effects of GelNB, samples of the PBS and GelNB groups were analyzed in depth. The abundance of characteristic values of the PBS and GelNB groups were screened through standard analysis. The Venn diagram showed that the characteristic values of the GelNB group (983 samples) were only 22.77% (281 samples) coinciding with that of the PBS group (953 samples) (Fig. 7D). To determine the changes in microbial species at different levels before and after GelNB treatment, we used linear discriminant analysis effect size (LEfSe) analysis to show the different species at all levels among groups. As shown in Fig. 7E, *Bacteroidetes* was the most dominant bacterium of GelNB at the phylum level, which has been proven to increase CD4$^+$ Foxp3+ to regulate cell abundance, thus stimulating epithelial repair through NF-κB-dependent signal transmission [65]. At the class level, *Gammaproteobacteria* was the most significant dominant bacterium [66], and *Bacilli* and *Erysipelotrichia* also showed significant abundance advantages. At the genus level, LEfSe analysis and barplot function not only verified the recovery effect of GelNB on *Lactobacillus* and *Muribaculaceae* levels, but also showed that *Prevotellaceae* was the dominant flora in the intestinal tract of IBD mice model. It has been reported that the abundance of this genus is negatively correlated with Th17 levels in peripheral blood, and Th17/Tregs balance has a predominant role in intestinal homeostasis (Fig. 7F) [67]. These results showed that GelNB could significantly restore the low abundance of beneficial bacteria caused by IBD at various levels, inhibiting the advantages of harmful bacteria, which played a key role in repairing epithelium and maintaining homeostasis.

Based on 16S rDNA sequencing results, we examined how these bacteria interact with GelNB and change the pathological status of IBD *in vivo*. IBD patients have a higher risk of *Clostridium* infection [68], which was also confirmed by our sequencing results (Fig. 7B). The results of the microbial culture experiment showed that the growth of *Clostridium* was significantly inhibited by the GelNB molecular coating environment (Fig. 7G). These results suggested that GelNB molecular coating might reduce susceptibility to *Clostridium* by effectively alleviating the progression of IBD. Another clinical study reported that the average level of *Bacteroides* in patients with active CD and UC was significantly lower than that in the normal control group, and an excessively low abundance of *Bacteroides* induced IBD [69]. Using bacterial culture, we found that the number of *Bacteroidetes* in the DSS-induced environment was very low, while the GelNB culture environment significantly restored its growth. In addition, the bacterial culture results also verified the low abundance level of probiotic *Lactobacillus* in DSS environment, and GelNB molecular coating could return it to normal.

Based on these findings, GelNB molecular coating demonstrated an ability to regulate intestinal microflora through the biological barrier function, promoting the development of intestinal microflora and accelerating the recovery of IBD. However, the specific mechanism by which microflora regulate IBD and how IBD recovery is accelerated remains to be explored. Therefore, based on the function prediction of PICRUSt2, we attempted to connect the intestinal flora with the physiological and biochemical functions related to the intestinal tract, so as to further verify that GelNB molecular coating acted as a biological barrier
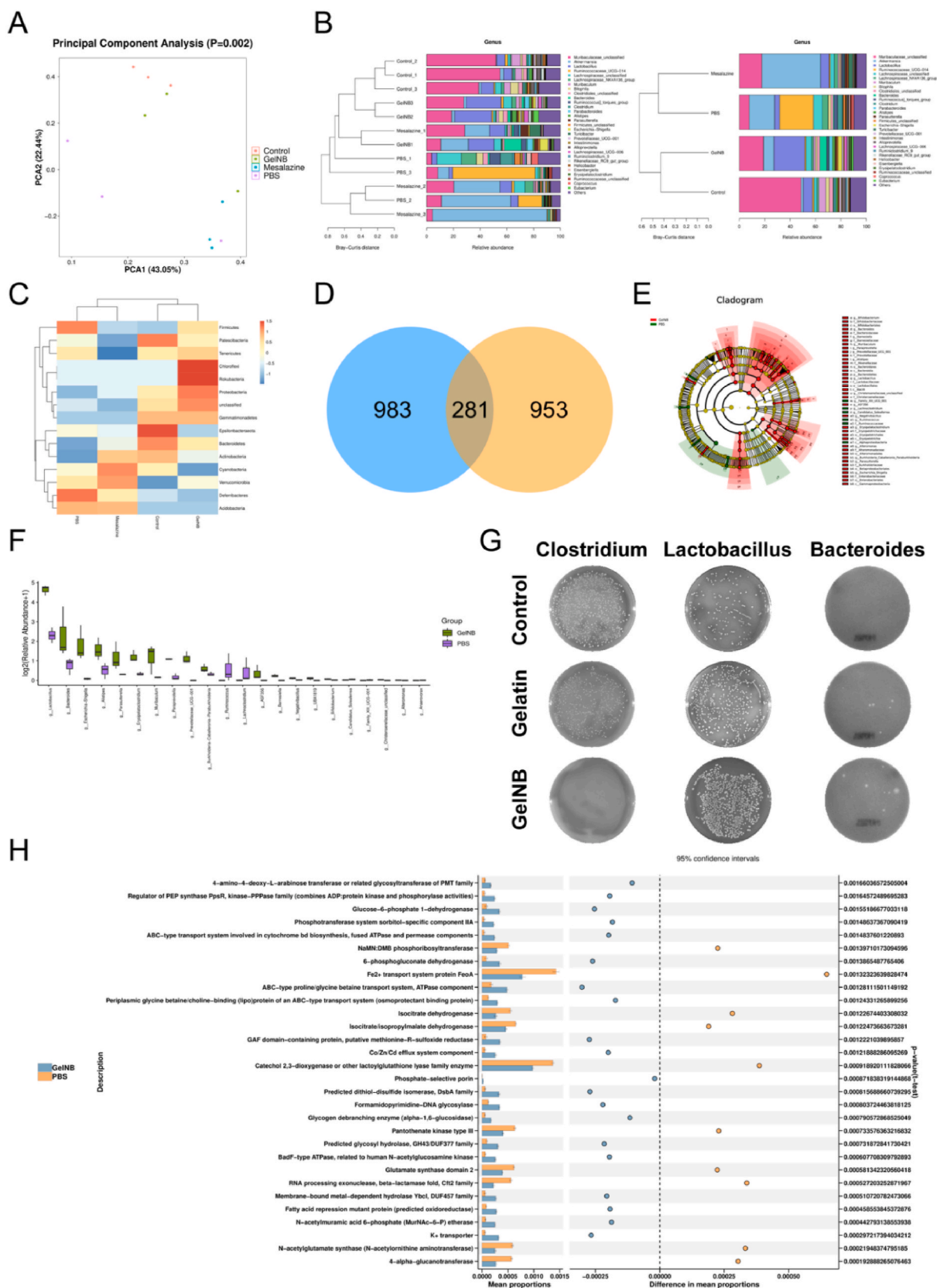
Fig. 7. GelNB molecular coating regulates the intestinal flora to realize the function of biological barrier action.
(A) PCA analyses of intestinal flora in negative control, Gelatin, Mesalazine and GelNB groups. **(B)** Cluster analysis results of the samples and groups intestinal flora at the genus level. **(C)** Heatmap of correlation analysis of intestinal flora in four groups. **(D)** Venn diagram of intestinal flora feature distribution in PBS group and GelNB group. **(E)** LEfSe analysis was performed to identify the differential bacteria composition in PBS group and GelNB group. **(F)** Barplot analysis revealed the bacterial relative abundance differences in PBS group and GelNB group. **(G)** The regulation of different bacterial activities of GelNB was shown by the spread plate method. **(H)** STAMP analysis predicted functional differences of bacteria in PBS group and GelNB group.

function to treat IBD. Fig. 7H showed the effect of GelNB molecular coating on the crucial links of metabolism and transport of glucose, amino acids, metal ions, and other substances *in vivo*. Among these substances, the expression levels of key enzymes involved in glycolysis, such as glucose-6-phosphate 1-dchydrogenase, 6-phosphogluconate dehydrogenase, glycogen branching enzyme (alpha-1,6-glycosylase), and glycosyl hydrolase, were significantly higher in GelNB than in PBS, which proved that GelNB molecular coating served multiple biological regulatory functions, promoting the transformation and metabolism of glucose, and reducing the adverse effects of glucose on inflammatory intestinal epithelium [70]. For amino acid transport, periplasmic glycine betaine/choline-binding (lipo)protein of an ABC-type transport system is an osmotic enhancer binding protein that was highly expressed in the GelNB-treated group, indicating that GelNB molecular coating promoted the infiltration of negatively charged glycine, together with glycine to relieve IBD by reducing the level of intestinal oxidative stress. In addition, the Fe^{2+} transport system FeoA was downregulated in the GelNB-treated group, which may have been caused by IBD-induced systemic iron-deficiency anemia. In addition, the compensatory increase in protein expression [71] and the decline of the protein level validated that the recovery of intestinal function was mostly promoted in the GelNB-treated group. Previous studies have found that there are substance metabolism [72] and transport [73] obstacles in IBD patients, which result in a deterioration of prognosis and an extension of the overall recovery time. Taken together, our results highlighted the biological barrier function of GelNB molecular coating for glucose, amino acids, and ions by regulating metabolism, transport, and other significant functions to protect against damage to intestinal function. Its specific action was likely to occur via promoting the growth of the intestine, improving the inflammatory environment, repairing the damaged mucosa, and strengthening the physical barrier.

In conclusion, GelNB is able to act as a biological barrier to regulate intestinal flora at all levels of microbial classification and restore it to the normal state. Functional analysis also suggests that this may be attributed to the regulation of GelNB on substance metabolism and transport. Therefore, we conclude that there is a close relationship between the biological barrier and the intestinal physical barrier, both of which cooperate in the intestinal microenvironment to regulate the development of IBD.

Severe IBD imposes a huge economic burden on national medical insurance, as well as the lives of the patients themselves. Therefore, the prevention of the occurrence of severe IBD is of great significance. The GelNB molecular coating developed in this study was found to prevent and treat IBD by forming a biophysical barrier on the intestinal surface to eliminate substance metabolism and intestinal microbial balance. Furthermore, this coating showed an enhanced performance in the prevention and treatment of severe IBD compared to the traditional clinical drug, metharazine. GelNB molecular coating is derived from biocompatible and economical Gelatin, which also has great advantages in promoting clinical transformation, helping to alleviate the suffering of patients, resulting in a more affordable process for diagnosis and treatment. However, it is worth mentioning that all of our animal models were administered enemas. Although a large number of biological agents are administered by enema, which has the advantages of maintaining the specific distribution of drugs [74] and facilitating tissue adhesion [75], it is associated with problems including poor tolerance [76], embarrassment, and reluctance of patients [77]. Therefore, we will continue to design and optimize the oral administration of GelNB in future works to broaden its clinical applications.

3. Methods

3.1. Synthesis and characterization

3.1.1. Synthesis of NB-COOH and obtainment of GelNB

NB was synthesized as previously reported [78]. Briefly, we first dissolved 4-hydroxy-3-(methoxy-D3) benzaldehyde, potassium carbonate, and 4-bromobutyric acid methyl ester in a ratio of 1:1.46:1.11 in dimethylformamide (DMF) and the mixture was deposited with chilled water. After drying, ipso was induced by substituting 4-(4-formyl-2-methoxyphenoxy methoxyphenyl) butanoic acid methyl ester by adding nitric acid (70%) for 3 h. To obtain the solid content, the ipso was filtered after being purified by DMF. TFA/H$_2$O in 1:10 v/v (100 mL) was added at 90 °C under reduced pressure and the whole product was dried out to obtain the yellow powder, which was later dissolved in THF/EtOH 1:1 v/v for 3 h. By dripping NaBH$_4$ slowly, the aqueous layer was collected by adding dichloromethane and drying over magnesium sulfate. To obtain NB-COOH, silica gel column chromatography with DCM/MeOH = 10:1 (1% TEA) was used in the purification process.

GelNB was dialyzed and lyophilized according to previously described methods [21]. GelNB was synthesized by adding Gelatin and carboxyl groups of NBCOOH into the reaction under the catalysis of 1-(3-Dimethylaminopropyl)-3-ethyl carbodiimide hydrochloride (EDC) (Aladdin, China) and *N*-hydroxy succinimide (NHS) (Aladdin) in dimethyl sulfoxide (DMSO, Sigma-Aldrich, USA). The mixture was carefully dripped into Gelatin solution (Sigma-Aldrich) and stirred at 45 °C for 4 h. Subsequently, the mixture was slowly dripped into a 10% w/v homogeneous Gelatin solution (Sigma-Aldrich) maintained at 37 °C and stirred at 45 °C for 4 h. After dialyzing the GelNB solution in distilled water for 72 h, the GelNB fraction was collected, lyophilized, and stored at 4 °C for further use [21].

3.1.2. Preparation and features of enema solution

The lyophilized GelNB foams were diluted with 1 × PBS at 37 °C to generate an enema solution at 100 mg/mL. After 1 min of UV light (365 nm, 30 mW/cm^2) activation, the solution was changed to an amino-reactive enema solution. Fourier transform infrared (FTIR)-attenuated total reflectance (ATR) spectroscopy analysis (Nicolet iS50; Thermo, USA) was applied to test the Gelatin solution, UV-activated Gelatin solution, un-activated GelNB solution, and UV-activated GelNB solution.

3.2. In vitro bowel wall modification and integration

3.2.1. SEM analysis for the characterization of GelNB on bowel

The enema solution was injected gently into the anus and pinched for 2 min to prevent effluence. The colon was resected from the euthanized mice and fixed with 2.5% glutaraldehyde overnight after washing three times with 1 × PBS. Liquid nitrogen was used to crack the colon into small pieces. After extraction with different concentrations of ethanol (50%, 70%, 80%, 90%, and 100% twice) for 10 min, all samples were observed under SEM (Nova Nano 450; Thermo) to compare the surface morphology.

3.2.2. Fluorescence evaluation for GelNB

Rhodamine B (RB) was incorporated in GelNB as a fluorescence indicator to quantify the adhesive ability of the coating on the bowel wall by referring to a previous study [79]. Rhodamine-labeled Gelatin (Rd-Gelatin) and GelNB were produced by mixing RB isothiocyanate with Gelatin and GelNB at 48 °C for two days. The lyophilized GelNB-RB foams were later dissolved at 37 °C to generate enema at a concentration of 100 mg/mL. The enema solution was injected into the anus, as described above. Fluorescence was detected using an IVIS Spectrum (PerkinElmer, USA) at 0, 8, 16, 24, 32, 40, and 48 h after enema.

3.2.3. Equilibrium dialysis experiments

GelNB-loaded molecular weight 3500 Da dialysis bags with deionized water were sealed by clips and immersed in 500 mL of D-Glucose (Meilunbio, China), L-arginine (Sangon Biotech, China), L-glutamic acid (Macklin, China), L-tryptophan (Macklin), glycine (Macklin), L-glutamine (Macklin), L-cysteine (Macklin), or Ringer's solution, respectively. As a control, deionized water was placed in a separate clean dialysis bag. The liquid in the dialysis bags was collected in a vacuum tube at regular

intervals as a dialysis test sample. The amino acid concentrations were determined using a total amino acid assay kit (Nanjing Jiancheng Bio-engineering Institute, China). The glucose concentration was assessed using a glucose colorimetric assay kit (Elabscience, China). The ion concentrations were measured using an automatic biochemical analyzer (Beckman Coulter AU5800, USA).

3.2.4. Validation of bacterial barrier property of the hydrogels

Bacterial cultures with a turbidity of 0.5 McFarland were inoculated onto $1 \times$ PBS, Gelatin solution, and GelNB solution. After culturing for about 12 h, the bacteria were further incubated for 12 h with agar plates. The number of bacterial colonies on the agar was counted.

3.3. In vitro cell experiment

3.3.1. Determination of mechanism underlying GelNB influence on cell viability and proliferation

NCM460, a common colonic mucosa cell line, was acquired from the Shanghai Cell Bank. The mouse macrophage cell line RAW 264.7 was obtained from ATCC. All cell lines were cultured in DMEM containing 10% FBS and 100 mg/mL penicillin-streptomycin (double antibody) at 37 °C in a 5% CO_2 incubator. Sterilized clean glass slides were immersed in 1% (3-Aminopropyl) triethoxysilane (Macklin) aqueous solution for half an hour and dried after [80]. Sterilized GelNB was added to the modified glass slides (30 mW/cm^2). After using UV to activate GelNB, cells were seeded at a density of 1×10^5 cells per well. Cell viability was measured using the live/dead staining assay and CCK-8 assay. A live-/dead staining assay was performed on days 0 and 3. CCK-8 assays were performed daily from day 1–3. The CCK-8 solution was diluted to 1:10 (v/v) in DMEM, and 100 μL of the mixture was added to each well and incubated at 37 °C for 1 h. The absorbance represented the living cells, which was measured at optical density at 450 nm with a microplate reader (Thermo MK3, USA).

3.4. Wound-scratch assay

Cell migration was measured using a wound scratch assay. Sterilized GelNB was added to the modified glass slides after UV irradiation (30 mW/cm^2). Approximately 1×10^5 NCM460 cells from each group were collected and seeded onto modified glass slides in 6-well plates. Two days after the cells reached the full plate, we used sterile pipette tips to scratch the wound from the top to the bottom across the middle of the wells. The cells were then washed twice with PBS to remove potential debris. Migrated areas were photographed every 12 h twice and were later measured using ImageJ software (National Institutes of Health, NIH, USA).

3.5. In vivo animal studies

3.5.1. Induction of IBD mice models and the treatment of IBD

Eight-week-old male C57 BL/6 (C57) mice were used for the experiments. All experiments were conducted in strict accordance with the institutional guidelines of the Zhejiang University School of Medicine Sir Run Run Shaw Hospital Animal Care and Use Committee, which conformed to the NIH Guide for the Care and Use of Laboratory Animals (ethical code SRRSH202107106). Colitis was induced by DSS (Yeason, China) or TNBS (Meilunbio) according to a previously described method [81,82].

DSS was dissolved in sterile distilled water at 50 mg/mL, and the control group mice drank sterile distilled water. Water was administered to the mice for seven days, which was replaced once every two days. The mice were fed with food and water ad libitum for five days. The enema solution was administered daily for 10 consecutive days, starting on the third day after colitis induction with DSS. On day 12, the mice were sacrificed.

TNBS (100 mg/kg) was dissolved in 50% ethanol. TNBS solution was slowly injected into the rectum of C57 mice via a catheter filled with a 1-mL syringe. Mice were placed in a vertical position for approximately 1 min to ensure that the therapeutic reagent could scatter homogeneously throughout the colon and cecum. The control group was administered a 50% ethanol solution. The mice were provided with food and water ad libitum for five days. The enema solution was administered daily for five consecutive days, starting on the third day after colitis induction with TNBS. Mice were sacrificed on day 7. The colon from the cecum to the anus was removed, and the length of each colon was recorded, after which each colon was washed in $1 \times$ PBS. Segments (0.5 cm) near the anus were removed for MPO activity measurements and RT-qPCR analysis. The remaining colon tissues were fixed in 4% formaldehyde for further histological and immunohistochemical analyses.

3.5.2. Clinical evaluation of IBD

The evaluation of DAI and colonic damage score was calculated for each animal as described by Fitzpatrick et al. [83,84] Each group of mice was observed daily during treatment, and changes in body weight, diarrhea, and bleeding conditions were recorded in a timely manner. Blood in the feces was tested using a hemoccult assay kit (Nanjing Jiancheng Bio-engineering Institute). DAI consisted of weight loss, diarrhea, and bloody stool scores. The colonic damage score was determined based on the infiltration and loss of goblet cells and crypts displayed in the sections.

3.5.3. Measurement of MPO activity

To measure the degree of inflammation in the colon, we used an MPO assay kit and tissue MPO to detect and quantify polymorphonuclear neutrophils using the Nanjing Jiancheng Bio-engineering Institute, according to the manufacturer's instructions.

3.5.4. Measurement of ROS release

The levels of ROS were detected through intraperitoneal injection of luminol to examine the severity of IBD (10 mg/kg, 5-amino-2,3-dihydro-1,4-phthalazinedione, Yeasen) using the IVIS Lumina Imaging System (PerkinElmer). A fixed-area region of interest (ROI) over the abdomen was generated to quantify the average radiance of the peak BLI signal [85].

3.5.5. Histology and immunohistochemical labelling

The fixed tissues were dehydrated and embedded in paraffin. Paraffin-embedded tissues were resected to obtain serial transverse histological sections, which were then stained with H&E. Alternative slides were deparaffinized and rehydrated through a series of ethanol (30%, 50%, 70%, 90%, and 100%) and xylene, followed by antigen retrieval in a spoiling water bath in citrate buffer (pH 6) for 10 min. Goat serum was used to block the samples for 30 min before being incubated with primary antibodies against Ki-67 (Abcam, USA), Occludin-1 (Abcam), or ZO-1 (Cell Signaling Technology) at 4 °C overnight. The secondary antibodies (Gene Tech Shanghai Company Limited, China) were incubated for 30 min. Images were taken using a NANO ZOOMER S60 (Hamamatsu, Japan). The IHC score was the product of the percentage of positive cells and staining intensity.

3.5.6. Quantitative RT-PCR

Total RNA was extracted from the cells or colons by adding TRIzol reagent (Invitrogen, USA) following the manufacturer's instructions, and oligo dT primers with reverse transcriptase (Yeason) were used to synthesize cDNA. Subsequently, real-time PCR was performed on a LightCycler® 480II (Roche, USA) in 10 μL of reaction volume using the Trans Start Green qPCR SuperMix Kit (Yeason). The $2^{-\Delta\Delta Ct}$ method was used to measure the relative mRNA fold changes. The primers used in our study are listed in Table S1.

3.5.7. Measurement of intestinal flora

To determine the gut microbial community, the flora of the intestinal

tract was assessed using 16S rDNA sequencing on DSS and control groups on day 12 [86]. Briefly, fresh feces (1 g) were collected from each mouse and stored in sterile tubes at −80 °C in an anaerobic environment. DNA from different fecal samples was extracted using the E.Z.N.A. ® Stool DNA Kit (D4015; Omega, Inc.). After elution in 50 μL of buffer, the DNA quality was detected by agarose gel electrophoresis and quantified using a UV spectrophotometer. Then, it was measured by PCR by LC-Bio Technology Co., Ltd. (Hangzhou, China) to build a cDNA library, which was assessed on an Agilent 2100 Bioanalyzer (Agilent, USA) and with the Library Quantification Kit for Illumina (Kapa Biosciences, USA), respectively. Raw data were synthesized by sequencing the libraries on the NovaSeq PE250 platform and were then analyzed to determine the diversity and abundance of the microbial population in the samples.

3.6. Statistical analysis

Statistical analysis was performed using IBM SPSS Statistics version 22 (IBM Corp., USA). Variables between groups were analyzed by Student's t-test and one-way ANOVA. The results are presented as the median $\pm$ standard error of the mean (SEM). Spearman or Pearson correlation was used for correlation analysis. Statistical significance was set at $P < 0.05$.

Funding

Data and materials availability

All data needed to evaluate the conclusions in the paper are present in the paper and/or the Supplementary Materials. Additional data related to this paper may be requested from the authors.

CRediT authorship contribution statement

Qijiang Mao: and performed most of the experiments, with the assistance from. **Haoqi Pan:** performed most of the experiments, with the assistance from. **Yiyin Zhang:** designed and improvement of hydrogel under the, Supervision, of. designed and improvement of hydrogel under the, Supervision, of, wrote the manuscript with input from. **Qiuwen Zhu:** designed and improvement of hydrogel under the supervision of. **Yi Hong:** participated in figure preparation. **Zhengze Huang:** designed and improvement of hydrogel under the, Supervision, of, wrote the manuscript with input from, and participated in figure preparation, All authors read and approved this version of manuscript. **Xu Feng:** designed and improvement of hydrogel under the, Supervision, of. **Yifeng Fang:** designed and improvement of hydrogel under the, Supervision, of. **WenChao Chen:** and designed and improvement of hydrogel under the, Supervision, of. **Pengfei Chen:** participated in figure preparation. **Bo Shen:** provided administrative support and revision suggestion. **Hongwei Ouyang:** conceived and designed the research. **Yuelong Liang:** and provided administrative support and revision suggestion, designed and improvement of hydrogel under the supervision of.

Declaration of competing interest

The authors declare that they have no known competing financial interests or personal relationships that could have appeared to influence the work reported in this paper.

Acknowledgments

Not applicable.

Appendix A. Supplementary data

Supplementary data to this article can be found online at https://doi.org/10.1016/j.bioactmat.2022.04.001.

References

[1] S. Danese, M. Argollo, C. Le Berre, L. Peyrin-Biroulet, JAK selectivity for inflammatory bowel disease treatment: does it clinically matter? Gut 68 (10) (2019) 1893–1899.

[2] M. Friedrich, M. Pohin, F. Powrie, Cytokine networks in the pathophysiology of inflammatory bowel disease, Immunity 50 (4) (2019).

[3] G.G. Kaplan, J.W. Windsor, The four epidemiological stages in the global evolution of inflammatory bowel disease, Nat. Rev. Gastroenterol. Hepatol. 18 (1) (2021) 56–66.

[4] D.C. Baumgart, W.J. Sandborn, Crohn's disease, Lancet 380 (9853) (2012) 1590–1605.

[5] L. Beaugerie, F. Carrat, J.-F. Colombel, A.-M. Bouvier, H. Sokol, A. Babouri, F. Carbonnel, D. Laharie, J.-L. Faucheron, T. Simon, A. de Gramont, L. Peyrin-Biroulet, Risk of new or recurrent cancer under immunosuppressive therapy in patients with IBD and previous cancer, Gut 63 (9) (2014) 1416–1423.

[6] G.G. Kaplan, The global burden of IBD: from 2015 to 2025, Nat. Rev. Gastroenterol. Hepatol. 12 (12) (2015) 720–727.

[7] G. Leccese, A. Bibi, S. Mazza, F. Facciotti, F. Caprioli, P. Landini, M. Paroni, Probiotic Lactobacillus and bifidobacterium strains counteract adherent-invasive (AIEC) virulence and hamper IL-23/Th17 Axis in ulcerative colitis, but not in crohn's disease, Cells 9 (8) (2020).

[8] W.-C. Lim, Y. Wang, J.K. MacDonald, S. Hanauer, Aminosalicylates for induction of remission or response in Crohn's disease, Cochrane Database Syst. Rev. 7 (2016), CD008870.

[9] S.C. Ng, A.N. Ananthakrishnan, New approaches along the IBD course: diet, tight control and stem cells, Nat. Rev. Gastroenterol. Hepatol. 16 (2) (2019) 82–84.

[10] J.F. Colombel, W.J. Sandborn, W. Reinisch, G.J. Mantzaris, A. Kornbluth, D. Rachmilewitz, S. Lichtiger, G. D'Haens, R.H. Diamond, D.L. Broussard, K. L. Tang, C.J. van der Woude, P. Rutgeerts, Infliximab, azathioprine, or combination therapy for Crohn's disease, N. Engl. J. Med. 362 (15) (2010) 1383–1395.

[11] J.-F. Colombel, P.J. Rutgeerts, W.J. Sandborn, M. Yang, A. Camez, P.F. Pollack, R. B. Thakkar, A.M. Robinson, N. Chen, P.M. Mulani, J. Chao, Adalimumab induces deep remission in patients with Crohn's disease, Clin. Gastroenterol. Hepatol. 12 (3) (2014).

[12] W.J. Sandborn, B.G. Feagan, P. Rutgeerts, S. Hanauer, J.-F. Colombel, B.E. Sands, M. Lukas, R.N. Fedorak, S. Lee, B. Bressler, I. Fox, M. Rosario, S. Sankoh, J. Xu, K. Stephens, C. Milch, A. Parikh, Vedolizumab as induction and maintenance therapy for Crohn's disease, N. Engl. J. Med. 369 (8) (2013) 711–721.

[13] A. Aprodu, J. Mantaj, B. Raimi-Abraham, D. Vllasaliu, Evaluation of a methylcellulose and hyaluronic acid hydrogel as a vehicle for rectal delivery of biologics, Pharmaceutics 11 (3) (2019).

[14] M. Neurath, Current and emerging therapeutic targets for IBD, Nat. Rev. Gastroenterol. Hepatol. 14 (11) (2017) 688.

[15] H.H. Arab, M.Y. Al-Shorbagy, D.M. Abdallah, N.N. Nassar, Telmisartan attenuates colon inflammation, oxidative perturbations and apoptosis in a rat model of experimental inflammatory bowel disease, PLoS One 9 (5) (2014), e97193.

[16] L.-J. Li, M.-Y. Li, Y.-T. Li, J.-J. Feng, F.-Q. Hao, Z. Lun, Adjuvant activity of Sargassum pallidum polysaccharides against combined Newcastle disease, infectious bronchitis and avian influenza inactivated vaccines, Mar. Drugs 10 (12) (2012) 2648–2660.

[17] M.J. Schuijs, S. Png, A.C. Richard, A. Tsyben, G. Hamm, J. Stockis, C. Garcia, S. Pinaud, A. Nicholls, X.R. Ros, J. Su, M.D. Eldridge, A. Riedel, E.M. Serrao, H.-R. Rodewald, M. Mack, J.D. Shields, E.S. Cohen, A.N.J. McKenzie, R.J.A. Goodwin, K.M. Brindle, J.C. Marioni, T.Y.F. Halim, ILC2-driven innate immune checkpoint mechanism antagonizes NK cell antimetastatic function in the lung, Nat. Immunol. 21 (9) (2020).

[18] T. Kobayashi, B. Siegmund, C. Le Berre, S.C. Wei, M. Ferrante, B. Shen, C. N. Bernstein, S. Danese, L. Peyrin-Biroulet, T. Hibi, Ulcerative colitis, Nat. Rev. Dis. Prim. 6 (1) (2020) 74.

[19] Z. Yan, F. He, F. Xiao, H. He, D. Li, L. Cong, L. Lin, H. Zhu, Y. Wu, R. Yan, X. Li, H. Shan, A semi-tryptic peptide centric metaproteomic mining approach and its potential utility in capturing signatures of gut microbial proteolysis, Microbiome 9 (1) (2021) 12.

[20] F. Crouwel, H.J.C. Buiter, N.K. de Boer, Gut microbiota-driven drug metabolism in inflammatory bowel disease, J. Crohns Colitis 15 (2) (2020) 307–315.

[21] Y. Zhang, C. Li, Q. Zhu, R. Liang, C. Xie, S. Zhang, Y. Hong, H. Ouyang, A long-term retaining molecular coating for corneal regeneration, Bioact. Mater. 6 (12) (2021) 4447–4454.

[22] Y. Hong, F. Zhou, Y. Hua, X. Zhang, C. Ni, D. Pan, Y. Zhang, D. Jiang, L. Yang, Q. Lin, Y. Zou, D. Yu, D.E. Arnot, X. Zou, L. Zhu, S. Zhang, H. Ouyang, A strongly adhesive hemostatic hydrogel for the repair of arterial and heart bleeds, Nat. Commun. 10 (1) (2019) 2060.

[23] Y. Niu, Q. Li, R. Xie, S. Liu, R. Wang, P. Xing, Y. Shi, Y. Wang, L. Dong, C. Wang, Modulating the phenotype of host macrophages to enhance osteogenesis in MSC-laden hydrogels: design of a glucomannan coating material, Biomaterials 139 (2017) 39–55.

[24] M. Pandey, H. Choudhury, S.K D/O Segar Singh, N. Chetty Annan, S. K. Bhattamisra, B. Gorain, M.C.I. Mohd Amin, Budesonide-loaded pectin/polyacrylamide hydrogel for sustained delivery: fabrication, characterization and in vitro release kinetics, Molecules 26 (9) (2021).

[25] Z. Guo, Y. Bai, Z. Zhang, H. Mei, J. Li, Y. Pu, N. Zhao, W. Gao, F. Wu, B. He, J. Xie, Thermosensitive polymer hydrogel as a physical shield on colonic mucosa for colitis treatment, J. Mater. Chem. B 9 (18) (2021) 3874–3884.

[26] L. Liu, W. Yao, Y. Rao, X. Lu, J. Gao, pH-Responsive carriers for oral drug delivery: challenges and opportunities of current platforms, Drug Deliv. 24 (1) (2017) 569–581.

[27] A.M. Dos Santos, S.G. Carvalho, A.B. Meneguin, R.M. Sábio, M.P.D. Gremião, M. Chorilli, Oral delivery of micro/nanoparticulate systems based on natural polysaccharides for intestinal diseases therapy: challenges, advances and future perspectives, J. Contr. Release 334 (2021) 353–366.

[28] R. Shoda, K. Matsueda, S. Yamato, N. Umeda, Epidemiologic analysis of Crohn disease in Japan: increased dietary intake of n-6 polyunsaturated fatty acids and animal protein relates to the increased incidence of Crohn disease in Japan, Am. J. Clin. Nutr. 63 (5) (1996) 741–745.

[29] P. Jantchou, S. Morois, F. Clavel-Chapelon, M.-C. Boutron-Ruault, F. Carbonnel, Animal protein intake and risk of inflammatory bowel disease: the E3N prospective study, Am. J. Gastroenterol. 105 (10) (2010) 2195–2201.

[30] N. Sakamoto, S. Kono, K. Wakai, Y. Fukuda, M. Satomi, T. Shimoyama, Y. Inaba, Y. Miyake, S. Sasaki, K. Okamoto, G. Kobashi, M. Washio, T. Yokoyama, C. Date, H. Tanaka, Dietary risk factors for inflammatory bowel disease: a multicenter case-control study in Japan, Inflamm. Bowel Dis. 11 (2) (2005) 154–163.

[31] M.C. Mentella, F. Scaldaferri, M. Pizzoferrato, A. Gasbarrini, G.A.D. Miggiano, Nutrition, IBD and gut microbiota: a review, Nutrients 12 (4) (2020).

[32] X. Ding, D. Li, M. Li, D. Tian, H. Yu, Q. Yu, Tumor necrosis factor-α acts reciprocally with solute carrier family 26, member 3, (downregulated-in-adenoma) and reduces its expression, leading to intestinal inflammation, Int. J. Mol. Med. 41 (3) (2018) 1224–1232.

[33] S. Torretta, A. Scagliola, L. Ricci, F. Mainini, S. Di Marco, I. Cuccovillo, A. Kajaste-Rudnitski, D. Sumpton, K.M. Ryan, S. Cardaci, D-mannose suppresses macrophage IL-1β production, Nat. Commun. 11 (1) (2020) 6343.

[34] E.A. Franzosa, A. Sirota-Madi, J. Avila-Pacheco, N. Fornelos, H.J. Haiser, S. Reinker, T. Vatanen, A.B. Hall, H. Mallick, L.J. McIver, J.S. Sauk, R.G. Wilson, B. W. Stevens, J.M. Scott, K. Pierce, A.A. Deik, K. Bullock, F. Imhann, J.A. Porter, A. Zhernakova, J. Fu, R.K. Weersma, C. Wijmenga, C.B. Clish, H. Vlamakis, C. Huttenhower, R.J. Xavier, Gut microbiome structure and metabolic activity in inflammatory bowel disease, Nat. Microbiol. 4 (2) (2019) 293–305.

[35] E.A. Scoville, M.M. Allaman, C.T. Brown, A.K. Motley, S.N. Horst, C.S. Williams, T. Koyama, Z. Zhao, D.W. Adams, D.B. Beaulieu, D.A. Schwartz, K.T. Wilson, L. A. Coburn, Alterations in lipid, amino acid, and energy metabolism distinguish crohn's disease from ulcerative colitis and control subjects by serum metabolomic profiling, Metabolomics 14 (1) (2018) 17.

[36] N. Li, P. Lewis, D. Samuelson, K. Liboni, J. Neu, Glutamine regulates Caco-2 cell tight junction proteins, Am. J. Physiol. Gastrointest. Liver Physiol. 287 (3) (2004) G726–G733.

[37] I. Tsune, K. Ikejima, M. Hirose, M. Yoshikawa, N. Enomoto, Y. Takei, N. Sato, Dietary glycine prevents chemical-induced experimental colitis in the rat, Gastroenterology 125 (3) (2003) 775–785.

[38] M. Davaatseren, J.-T. Hwang, J.H. Park, M.-S. Kim, S. Wang, M.J. Sung, Poly-γ-glutamic acid attenuates angiogenesis and inflammation in experimental colitis, 2013, Mediat. Inflamm. (2013), 982383.

[39] M.F. Neurath, S.P.L. Travis, Mucosal healing in inflammatory bowel diseases: a systematic review, Gut 61 (11) (2012) 1619–1635.

[40] A.K. Gaharwar, I. Singh, A. Khademhosseini, Engineered biomaterials for in situ tissue regeneration, Nat. Rev. Mater. 5 (9) (2020) 686–705.

[41] D.Y. Shu, A.E.K. Hutcheon, J.D. Zieske, X. Guo, Epidermal growth factor stimulates transforming growth factor-beta receptor type II expression in corneal epithelial cells, Sci. Rep. 9 (1) (2019) 8079.

[42] J. Reiser, W. Kriz, M. Kretzler, P. Mundel, The glomerular slit diaphragm is a modified adherens junction, J. Am. Soc. Nephrol. 11 (1) (2000) 1–8.

[43] S. Zhang, Y. Liu, X. Zhang, D. Zhu, X. Qi, X. Cao, Y. Fang, Y. Che, Z.-C. Han, Z.-X. He, Z. Han, Z. Li, Prostaglandin E hydrogel improves cutaneous wound healing via M2 macrophages polarization, Theranostics 8 (19) (2018) 5348–5361.

[44] J. Chen, J. Yang, R. Liu, C. Qiao, Z. Lu, Y. Shi, Z. Fan, Z. Zhang, X. Zhang, Dual-targeting theranostic system with mimicking apoptosis to promote myocardial infarction repair modulation of macrophages, Theranostics 7 (17) (2017) 4149–4167.

[45] X. Cao, L. Duan, H. Hou, Y. Liu, S. Chen, S. Zhang, Y. Liu, C. Wang, X. Qi, N. Liu, Z. Han, D. Zhang, Z.-C. Han, Z. Guo, Q. Zhao, Z. Li, IGF-1C hydrogel improves the therapeutic effects of MSCs on colitis in mice through regulating the activation M2 macrophage polarization, Theranostics 10 (17) (2020) 7697–7709.

[46] J.-C. Lin, J.-Q. Wu, F. Wang, F.-Y. Tang, J. Sun, B. Xu, M. Jiang, Y. Chu, D. Chen, X. Li, S. Su, Y. Zhang, N. Wu, S. Yang, K. Wu, J. Liang, QingBai decoction regulates intestinal permeability of dextran sulphate sodium-induced colitis through the modulation of notch and NF-κB signalling, Cell Prolif 52 (2) (2019), e12547.

[47] P.-D. Lu, Y.-H. Zhao, Targeting NF-κB pathway for treating ulcerative colitis: comprehensive regulatory characteristics of Chinese medicines, Chin. Med. 15 (2020) 15.

[48] W. Kim, D. Kim, S. Jeong, S. Ju, H. Lee, S. Kim, J.-W. Yoo, I.-S. Yoon, Y. Jung, Conjugation of amisulpride, an anti-psychotic agent, with 5-aminosalicylic acid via an azo bond yields an orally active mutual prodrug against rat colitis, Pharmaceutics 11 (11) (2019).

[49] E.-M. Bleich, M. Martin, A. Bleich, A. Klos, The Mongolian gerbil as a model for inflammatory bowel disease, Int. J. Exp. Pathol. 91 (3) (2010) 281–287.

[50] S. Regmi, Y. Seo, J.-S. Ahn, S. Pathak, S. Acharya, T.T. Nguyen, S. Yook, J.-H. Sung, J.-B. Park, J.O. Kim, C.S. Young, H.-S. Kim, J.-H. Jeong, Heterospheroid formation improves therapeutic efficacy of mesenchymal stem cells in murine colitis through immunomodulation and epithelial regeneration, Biomaterials 271 (2021) 120752.

[51] L. Bronsart, L. Nguyen, A. Habtezion, C. Contag, Reactive oxygen species imaging in a mouse model of inflammatory bowel disease, Mol. Imag. Biol. 18 (4) (2016) 473–478.

[52] H. Kim, Y. Kim, I.-H. Kim, K. Kim, Y. Choi, ROS-responsive activatable photosensitizing agent for imaging and photodynamic therapy of activated macrophages, Theranostics 4 (1) (2013).

[53] J. Du, Y. Chen, Y. Shi, T. Liu, Y. Cao, Y. Tang, X. Ge, H. Nie, C. Zheng, Y.C. Li, 1,25-Dihydroxyvitamin D protects intestinal epithelial barrier by regulating the myosin light chain kinase signaling pathway, Inflamm. Bowel Dis. 21 (11) (2015) 2495–2506.

[54] F. Sánchez de Medina, I. Romero-Calvo, C. Mascaraque, O. Martínez-Augustin, Intestinal inflammation and mucosal barrier function, Inflamm. Bowel Dis. 20 (12) (2014) 2394–2404.

[55] A. Lima Martins, R.A. Volpato, M.d.P. Zago-Gomes, The prevalence and phenotype in Brazilian patients with inflammatory bowel disease, BMC Gastroenterol. 18 (1) (2018) 87.

[56] C.-T. Chiu, S.-N. Kuo, S.-W. Hung, C.-Y. Yang, Combined treatment with hyaluronic acid and mesalamine protects rats from inflammatory bowel disease induced by intracolonic administration of trinitrobenzenesulfonic acid, Molecules 22 (6) (2017).

[57] M.F. Neurath, I. Fuss, B.L. Kelsall, E. Stüber, W. Strober, Antibodies to interleukin 12 abrogate established experimental colitis in mice, J. Exp. Med. 182 (5) (1995) 1281–1290.

[58] T. Araki, K. Mitsuyama, H. Yamasaki, M. Morita, K. Tsuruta, A. Mori, T. Yoshimura, S. Fukunaga, K. Kuwaki, S. Yoshioka, H. Takedatsu, T. Kakuma, J. Akiba, T. Torimura, Therapeutic potential of a self-assembling peptide hydrogel to treat colonic injuries associated with inflammatory bowel disease, J. Crohns Colitis 15 (9) (2021) 1517–1527.

[59] S.M. Lee, N.-H. Kim, S. Lee, Y.N. Kim, J.-D. Heo, J.-R. Rho, E.J. Jeong, 10)-Debromohymenialdisine from marine sponge sp. regulates intestinal inflammatory responses in Co-culture model of epithelial caco-2 cells and THP-1 macrophage cells, Molecules 24 (18) (2019).

[60] Y. Chen, B. Yang, R.P. Ross, Y. Jin, C. Stanton, J. Zhao, H. Zhang, W. Chen, Orally administered CLA ameliorates DSS-induced colitis in mice via intestinal barrier improvement, oxidative stress reduction, and inflammatory cytokine and gut microbiota modulation, J. Agric. Food Chem. 67 (48) (2019) 13282–13298.

[61] E. Dellaporta, L.-D. Lazaridis, V. Koussoulas, M.G. Netea, E.J. Giamarellos-Bourboulis, K. Triantafyllou, Association between genotypes of rs34436714 of NLRP12 and serum tumor necrosis factor-alpha in inflammatory bowel disease: a case-control study, Medicine (Baltim.) 98 (23) (2019), e15913.

[62] L. Zhang, S. Gui, Y. Xu, J. Zeng, J. Wang, Q. Chen, L. Su, Z. Wang, R. Deng, F. Chu, W. Liu, X. Jin, X. Lu, Colon tissue-accumulating mesoporous carbon nanoparticles loaded with cecropin for ulcerative colitis therapy, Theranostics 11 (7) (2021) 3417–3438.

[63] J. Lloyd-Price, C. Arze, A.N. Ananthakrishnan, M. Schirmer, J. Avila-Pacheco, T. W. Poon, E. Andrews, N.J. Ajami, K.S. Bonham, C.J. Brislawn, D. Casero, H. Courtney, A. Gonzalez, T.G. Graeber, A.B. Hall, K. Lake, C.J. Landers, H. Mallick, D.R. Plichta, M. Prasad, G. Rahnavard, J. Sauk, D. Shungin, Y. Vázquez-Baeza, R.A. White, J. Braun, L.A. Denson, J.K. Jansson, R. Knight, S. Kugathasan, D. P.B. McGovern, J.F. Petrosino, T.S. Stappenbeck, H.S. Winter, C.B. Clish, E. A. Franzosa, H. Vlamakis, R.J. Xavier, C. Huttenhower, Multi-omics of the gut microbial ecosystem in inflammatory bowel diseases, Nature 569 (7758) (2019) 655–662.

[64] Y. Liu, H. Fang, H. Liu, H. Cheng, L. Pan, M. Hu, X. Li, Goji berry juice fermented by probiotics attenuates dextran sodium sulfate-induced ulcerative colitis in mice, J. Funct.Foods 83 (2021), 104491.

[65] E. Bellaguarda, E.B. Chang, IBD and the gut microbiota–from bench to personalized medicine, Curr. Gastroenterol. Rep. 17 (4) (2015) 15.

[66] H.-C. Zhu, X.-K. Jia, Y. Fan, S.-H. Xu, X.-Y. Li, M.-Q. Huang, M.-L. Lan, W. Xu, S.-S. Wu, Alisol B 23-acetate ameliorates azoxymethane/dextran sodium sulfate-induced male murine colitis-associated colorectal cancer modulating the composition of gut microbiota and improving intestinal barrier, Front. Cell. Infect. Microbiol. 11 (2021), 640225.

[67] F. Zhu, H. Li, Y. Liu, C. Tan, X. Liu, H. Fan, H. Wu, Y. Dong, T. Yu, S. Chu, H. He, X. Zhu, miR-155 antagomir protect against DSS-induced colitis in mice through regulating Th17/Treg cell balance by Jarid2/Wnt/β-catenin, Biomed. Pharmacother. 126 (2020), 109909.

[68] A. Anderson, B. Click, C. Ramos-Rivers, D. Cheng, D. Babichenko, I. E. Koutroubakis, J.G. Hashash, M. Schwartz, J. Swoger, A.M. Barrie, M.A. Dunn, M. Regueiro, D.G. Binion, Lasting impact of Clostridium difficile infection in inflammatory bowel disease: a propensity score matched analysis, Inflamm. Bowel Dis. 23 (12) (2017) 2180–2188.

[69] H. Zafar, M.H. Saier, Gut species in health and disease, Gut Microb. 13 (1) (2021).

[70] S. Khan, S. Waliullah, V. Godfrey, M.A.W. Khan, R.A. Ramachandran, B. L. Cantarel, C. Behrendt, L. Peng, L.V. Hooper, H. Zaki, Dietary simple sugars alter

microbial ecology in the gut and promote colitis in mice, Sci. Transl. Med. 12 (567) (2020).

[71] F. de la Morena, J.P. Gisbert, [Anemia and inflammatory bowel disease], Rev. Esp. Enferm. Dig. 100 (5) (2008) 285–293.

[72] Z. Zhang, H. Tang, P. Chen, H. Xie, Y. Tao, Demystifying the manipulation of host immunity, metabolism, and extraintestinal tumors by the gut microbiome, Signal Transduct. Targeted Ther. 4 (2019) 41.

[73] J.H. Ye, V.M. Rajendran, Adenosine: an immune modulator of inflammatory bowel diseases, World J. Gastroenterol. 15 (36) (2009) 4491–4498.

[74] S. Zhang, L. Kang, S. Hu, J. Hu, Y. Fu, Y. Hu, X. Yang, Carboxymethyl chitosan microspheres loaded hyaluronic acid/Gelatin hydrogels for controlled drug delivery and the treatment of inflammatory bowel disease, Int. J. Biol. Macromol. 167 (2021) 1598–1612.

[75] S. Zhang, J. Ermann, M.D. Succi, A. Zhou, M.J. Hamilton, B. Cao, J.R. Korzenik, J. N. Glickman, P.K. Vemula, L.H. Glimcher, G. Traverso, R. Langer, J.M. Karp, An inflammation-targeting hydrogel for local drug delivery in inflammatory bowel disease, Sci. Transl. Med. 7 (300) (2015), 300ra128.

[76] F. Seibold, N. Fournier, C. Beglinger, C. Mottet, V. Pittet, G. Rogler, Topical therapy is underused in patients with ulcerative colitis, J. Crohns Colitis 8 (1) (2014) 56–63.

[77] T.M. Goodsall, S.P. Costello, R.V. Bryant, ABC of topical therapy in inflammatory bowel disease, JGH Open 4 (4) (2020) 556–557.

[78] Y. Yang, J. Zhang, Z. Liu, Q. Lin, X. Liu, C. Bao, Y. Wang, L. Zhu, Tissue-integratable and biocompatible photogelation by the imine crosslinking reaction, Adv. Mater. 28 (14) (2016) 2724–2730.

[79] H. Tan, D. Huang, L. Lao, C. Gao, RGD modified PLGA/Gelatin microspheres as microcarriers for chondrocyte delivery, J. Biomed. Mater. Res. B Appl. Biomater. 91 (1) (2009) 228–238.

[80] H. Li, Y. Xia, J. Wu, Q. He, X. Zhou, G. Lu, L. Shang, F. Boey, S.S. Venkatraman, H. Zhang, Surface modification of smooth poly(L-lactic acid) films for Gelatin immobilization, ACS Appl. Mater. Interfaces 4 (2) (2012) 687–693.

[81] C. Trilleaud, V. Gauttier, K. Biteau, I. Girault, L. Belarif, C. Mary, S. Pengam, G. Teppaz, V. Thepenier, R. Danger, G. Robert-Siegwald, M. Néel, S. Bruneau, A. Glémain, A. Néel, A. Poupon, J.F. Mosnier, G. Chêne, M. Dubourdeau, G. Blancho, B. Vanhove, N. Poirier, Agonist anti-ChemR23 mAb reduces tissue neutrophil accumulation and triggers chronic inflammation resolution, Sci. Adv. 7 (14) (2021).

[82] N. He, X. Chen, D. Wang, K. Xu, L. Wu, Y. Liu, H. Tao, Q. Zhao, X. Cao, Y. Li, N. Liu, X. Qi, Z. Han, D. Kong, J. Yang, Z. Li, VE-Cadherin regulates the self-renewal of mouse embryonic stem cells via LIF/Stat3 signaling pathway, Biomaterials 158 (2018) 34–43.

[83] L.R. Fitzpatrick, J. Wang, T. Le, In vitro and in vivo effects of gliotoxin, a fungal metabolite: efficacy against dextran sodium sulfate-induced colitis in rats, Dig. Dis. Sci. 45 (12) (2000) 2327–2336.

[84] G. Can, S. Ayvaz, H. Can, S. Demirtas, H. Aksit, B. Yilmaz, U. Korkmaz, M. Kurt, T. Karaca, The syk inhibitor fostamatinib decreases the severity of colonic mucosal damage in a rodent model of colitis, J. Crohns Colitis 9 (10) (2015) 907–917.

[85] J.-C. Tseng, A.L. Kung, In vivo imaging of inflammatory phagocytes, Chem. Biol. 19 (9) (2012) 1199–1209.

[86] J.-P. Furet, O. Firmesse, M. Gourmelon, C. Bridonneau, J. Tap, S. Mondot, J. Doré, G. Corthier, Comparative assessment of human and farm animal faecal microbiota using real-time quantitative PCR, FEMS Microbiol. Ecol. 68 (3) (2009) 351–362.